

Western  Graduate&PostdoctoralStudies

Western University
Scholarship@Western

Electronic Thesis and Dissertation Repository

4-23-2012 12:00 AM

Enabling Techniques Design for QoS Provision in Wireless Communications

Penghui Mi
The University of Western Ontario

Supervisor
Dr. Xianbin Wang
The University of Western Ontario

Graduate Program in Electrical and Computer Engineering
A thesis submitted in partial fulfillment of the requirements for the degree in Master of Engineering Science
© Penghui Mi 2012

Follow this and additional works at: <https://ir.lib.uwo.ca/etd>



Part of the [Systems and Communications Commons](#)

Recommended Citation

Mi, Penghui, "Enabling Techniques Design for QoS Provision in Wireless Communications" (2012).
Electronic Thesis and Dissertation Repository. 436.
<https://ir.lib.uwo.ca/etd/436>

This Dissertation/Thesis is brought to you for free and open access by Scholarship@Western. It has been accepted for inclusion in Electronic Thesis and Dissertation Repository by an authorized administrator of Scholarship@Western. For more information, please contact wlsadmin@uwo.ca.

Enabling Techniques Design for QoS Provision in Wireless Communications

(Spine title: QoS Guarantees in Modern Communication Systems)

(Thesis format: Monograph)

by

Penghui Mi

**Graduate Program
in
Engineering Science
Department of Electrical and Computer Engineering**

**A thesis submitted in partial fulfillment
of the requirements for the degree of
Master of Engineering Science**

**The School of Graduate and Postdoctoral Studies
The University of Western Ontario
London, Ontario, Canada**

© Penghui Mi 2012

THE UNIVERSITY OF WESTERN ONTARIO
SCHOOL OF GRADUATE AND POSTDOCTORAL STUDIES
CERTIFICATE OF EXAMINATION

Chief Advisor:

Dr. Xianbin Wang

Examining Board:

Dr. Evgueni Bordatchev

Advisory Committee:

Dr. Jagath Samarabandu

Dr. Weiming Shen

The thesis by

Penghui Mi

entitled:

Enabling Techniques Design for QoS Provision in Wireless Communications

is accepted in partial fulfillment of the

requirements for the degree of

Master of Engineering Science

Date: _____

Chair of Examining Board
Dr. R. K. Rao

Abstract

Guaranteeing Quality of Service (QoS) has become a recognized feature in the design of wireless communications. In this thesis, the problem of QoS provision is addressed from different perspectives in several modern communication systems.

In the first part of the thesis, a wireless communication system with the base station (BS) associated by multiple subscribers (SS) is considered, where different subscribers require different QoS. Using the cross-layer approach, the conventional single queue finite state Markov chain system model is extended to multiple queues' scenario by combining the MAC layer queue status with the physical layer channel states, modeled by finite state Markov channel (FSMC). To provide the diverse QoS to different subscribers, a priority-based rate allocation (PRA) algorithm is proposed to allocate the physical layer transmission rate to the multiple medium access control (MAC) layer queues, where different queues are assigned with different priorities, leading to their different QoS performance and thus, the diverse QoS are guaranteed.

Then, the subcarrier allocation in multi-user OFDM (MU-OFDM) systems is studied, constrained by the MAC layer diverse QoS requirements. A two-step cross-layer dynamic subcarrier allocation algorithm is proposed where the MAC layer queue status is firstly modeled by a finite state Markov chain, using which MAC layer diverse QoS constraints are transformed to the corresponding minimum physical layer data rate of each user. Then, with the purpose of maximizing the system capacity, the physical layer OFDM subcarriers are allocated to the multiple users to satisfy their minimum data rate requirements, which is derived by the MAC layer queue status model.

Finally, the problem of channel assignment in IEEE 802.11 wireless local area networks (WLAN) is investigated, oriented by users' QoS requirements. The number of users in the IEEE 802.11 channels is first determined through the number of different channel impulse responses (CIR) estimated at physical layer. This information is involved thereafter in the proposed channel assignment algorithm, which aims at maximum system throughput, where we explore the partially overlapped IEEE 802.11 channels to provide additional frequency resources. Moreover, the users' QoS requirements are set to trigger the channel assignment process, such that the system can constantly maintain the required QoS.

Acknowledgements

First, and foremost, I would like to express my genuine and sincere gratitude to my supervisor, Prof. Xianbin Wang for his guidance, support and encouragement in the developing of my research. It was him who brought me into the filed of wireless communications and without his vision, deep insight, valuable advices and continuous supports, this work would never have been possible. It is an great honor for me to join this research group and work with him. This journey is proven to be enjoyable and rewarding.

Sincere thanks to Dr. Evgueni Bordatchev, Dr. Jagath Samarabandu and Dr. Weiming Shen for joining in my committee as well as their valuable time and constructive suggestions.

I would also like to thank the faculties, stuffs and students I met in The University of Western Ontario, who have helped me directly or indirectly in completing my studies.

As always, I deeply own my thanks to my parents and my sister for their love and support throughout this degree and my life.

Table of Contents

Certificate of Examination	ii
Abstract	iii
Acknowledgements	v
List of tables	x
List of figures	xi
Acronyms	xiii
1 Introduction	1
1.1 Research Motivations	1
1.2 Research Objectives	2
1.3 Thesis Contributions	3
1.4 Thesis Organization	4
2 Basic Concepts Preview	6
2.1 Discrete-time Markov Chains	6
2.1.1 Definition	6
2.1.2 State Transition Probability Formulation	6
2.1.3 State Probability Formulation	8
2.1.4 Steady-state Behavior	9
2.1.4.1 Ergodic Markov chain	9
2.1.4.2 Stationary distribution of Markov chain	9
2.2 Queueing System	10
2.2.1 Input Process	10
2.2.2 System Structure	11

Table of Contents

2.2.3	Output Process	12
2.2.4	Kendall Notation	13
2.3	OFDM System	13
2.3.1	Concept of OFDM	13
2.3.2	OFDM Transmitter	15
2.3.3	OFDM Receiver	17
2.3.4	Advantages and Disadvantages of OFDM systems	18
2.4	IEEE 802.11 WLAN	20
2.4.1	Overview of WLAN	20
2.4.2	The PHY and MAC of WLAN	21
2.4.2.1	The physical layer	21
2.4.2.2	The media access control layer	21
2.5	Summary	24
3	Modeling of Wireless Communications for Diverse QoS Provision	25
3.1	Introduction	25
3.2	System Model	27
3.2.1	System Description	27
3.2.2	Adaptive Modulation and Coding	30
3.2.3	Finite State Markov Channel	32
3.2.3.1	Channel partitionings	33
3.2.3.2	Channel state transition probabilities	35
3.3	Proposed Multiple Queue Finite State Markov Chain System Model	37
3.3.1	Queue Behavior Modeling	37
3.3.2	Priority-Based Rate Allocation	38
3.3.3	System Modeling Using Finite State Markov Chain	40
3.3.3.1	Derivation of state transition matrix	40
3.3.3.2	Stationary distribution of Markov chain	41
3.4	System QoS Performance	41
3.4.1	Packet Loss Rate	42
3.4.2	Average System Delay	43
3.5	Simulations	44
3.5.1	Parameter Setting	44
3.5.2	Simulation Results	44

Table of Contents

3.6	Summary	48
4	QoS Constrained Subcarrier Allocation in MU-OFDM system	49
4.1	Introduction	49
4.2	System Model	51
4.3	Problem Formulation	52
4.4	Proposed Cross-Layer Dynamic Subcarrier Allocation	54
4.4.1	MAC Layer Queue Status Model	54
4.4.1.1	Queuing model using finite state Markov Chain	54
4.4.1.2	QoS performance analysis	55
4.4.2	Dynamic Subcarrier Allocation at Physical Layer	56
4.5	Simulations	59
4.5.1	Parameter Setting	59
4.5.2	MAC Layer Queue Performance	59
4.5.3	Physical Layer Subcarrier Allocation Performance	61
4.6	Summary	63
5	QoS Oriented Channel Assignment in IEEE 802.11 WLANs	64
5.1	Introduction	64
5.2	System Model	67
5.3	CIR-Based User Number Estimation	68
5.3.1	Physical Layer Model	68
5.3.2	LS Channel Estimation	69
5.3.3	Mitigation of CIR Estimation Noise	70
5.3.4	Hypothesis Testing for CIR Differentiation	72
5.3.5	Adaptive CIR Determination Threshold	73
5.3.6	Details of the CIR-Based Estimation Algorithm	74
5.4	Channel Assignment Exploiting IEEE 802.11 Partially Overlapped Channels	76
5.4.1	Interference Analysis of Partially Overlapped Channels	76
5.4.2	Problem Formulation	78
5.4.3	Interference Factor (I-factor) Calculation	80
5.4.4	Implementation of the Proposed Channel Assignment Algorithm	81
5.5	Simulations	82
5.5.1	Parameter Setting	82
5.5.2	Adaptive Noise Elimination and CIR Determination Thresholds	82

Table of Contents

5.5.3	Accuracy Analysis of CIR-based User Number Estimation	84
5.5.4	IEEE 802.11 WLAN System Performance Improvement	85
5.6	Summary	87
6	Conclusion and Future Work	88
6.1	Conclusion	88
6.2	Future Work	89
	References	91
	Curriculum Vitae	98

List of Tables

3.1	Transmission Modes with Uncoded M_n -QAM Modulation	31
3.2	Transmission Modes with Conventionally Coded Modulation	31
5.1	Simulation Parameters for User Number Estimation	82
5.2	IEEE 802.11 System Parameters	83

List of Figures

2.1	State transition diagram of discrete-time Markov chain.	7
2.2	Periodic Markov chain.	9
2.3	Schematic diagram of a queueing system.	10
2.4	System structure of a queueing system: parallel servers.	11
2.5	System structure of a queueing system: serial servers.	12
2.6	The structure of OFDM symbol with cyclic prefix.	16
2.7	Block diagram of OFDM transmitter.	16
2.8	Constellation diagram for rectangular 16-QAM.	17
2.9	Block diagram of OFDM receiver.	18
2.10	Elimination of ISI through cyclic prefix.	18
2.11	Bandwidth utilization comparison between the OFDM system and the conventional FDM system [7].	19
2.12	IEEE 802.11 MAC architecture.	22
2.13	CSMA/CA basic access mechanism.	22
2.14	CSMA/CA CTS/RTS mechanism.	23
3.1	Wireless communication system diagram with a base station associated by multiple subscribers	28
3.2	Wireless link from the base station (BS) to a subscriber (SS)	28
3.3	Physical layer frame structure	29
3.4	Channel partitioning in FSMC [38]	33
3.5	$N + 1$ finite state Markov channel	35
3.6	Packet loss rate under different pre-defined packet error rates.	45
3.7	Average system delay under different pre-defined packet error rates.	46
3.8	Packet loss rate under different traffic loads.	46
3.9	Average system delay under different traffics loads.	47
4.1	Multiuser OFDM system.	51
4.2	Packet loss rate under different physical layer data rates.	60

List of Figures

4.3	MAC layer average queue size under different physical layer data rates. . .	61
4.4	Normalized ergodic sum capacity distribution among users.	62
5.1	Typical infrastructure-based IEEE 802.11 WLAN with AP transmission range overlap.	67
5.2	Threshold to eliminate the environment noise.	71
5.3	IEEE 802.11 channels in the 2.4GHz ISM band [68].	76
5.4	Transmit spectrum mask for IEEE 802.11 OFDM modulation.	77
5.5	Theoretical I-factor on 2.4GHz 802.11 channels with OFDM modulation. .	80
5.6	Noise elimination threshold under different path number and SNR combinations.	83
5.7	CIR determination threshold under different path number and SNR combinations.	84
5.8	CDF of the estimation errors under different SNR situations.	85
5.9	MAC layer packet drop rate under different packet arrival rates with different AP numbers.	86
5.10	Average system throughput under different packet arrival rates with different AP numbers.	86

Acronyms

ACK	<i>Acknowledgement</i>
ADC	<i>Analog-to-Digital Converter</i>
AWGN	<i>Additive White Gaussian Noise</i>
A/D	<i>Analog-to-Digital</i>
AMC	<i>Adaptive Modulation and Coding</i>
AP	<i>Access Point</i>
AR-1	<i>Autoregressive model of order 1</i>
BER	<i>Bit-Error-Rate</i>
BS	<i>Base Station</i>
CDF	<i>Cumulative Distribution Function</i>
CFO	<i>Carrier Frequency Offset</i>
CIR	<i>Channel Impulse Response</i>
CP	<i>Cyclic Prefix</i>
CSI	<i>Channel State Information</i>
CSMA/CA	<i>Carrier Sense Multiple Access with Collision Avoidance</i>
CTS	<i>Clear To Send</i>
DAC	<i>Digital-to-Analog Converter</i>
D/A	<i>Digital-to-Analog</i>
DCF	<i>Distributed Coordination Function</i>
DIFS	<i>Distributed Interframe Space</i>
DSSS	<i>Direct Sequence Spread Spectrum</i>
ETSI	<i>European Telecommunications Standards Institute</i>
EUN	<i>Equivalent User Number</i>
FCFS	<i>First-Come-First-Served</i>
FDM	<i>Frequency Division Multiplexing</i>
FEC	<i>Forward Error Coding</i>
FFT	<i>Fast Fourier transform</i>
FHSS	<i>Frequency Hopping Spread Spectrum</i>

FIFO	<i>First-In-First-Out</i>
FSMC	<i>Finite State Markov Channel</i>
HiperLAN	<i>High performance radio Local Area Network</i>
IDFT	<i>Inverse Discrete Fourier Transform</i>
IFFT	<i>Inverse Fast Fourier Transform</i>
IR	<i>Infrared Light</i>
ISI	<i>Intersymbol Interference</i>
ISM	<i>Industrial, Scientific, and Medical</i>
LCFS	<i>Last-Come-First-Served</i>
LCR	<i>Level Crossing Rate</i>
LS	<i>Least Square</i>
MAC	<i>Medium Access Control</i>
MSE	<i>Mean Squared Error</i>
MIMO	<i>Multiple-Input Multiple-Output</i>
MU-OFDM	<i>Multi-user OFDM</i>
NAV	<i>Network Allocation Vector</i>
OFDM	<i>Orthogonal Frequency Division Multiplexing</i>
PAPR	<i>Peak-to-Average Power Ratio</i>
PDF	<i>Probability Density Function</i>
PER	<i>Packet Error Rate</i>
PRA	<i>Priority-based Rate Allocation</i>
PCF	<i>Point Coordination Function</i>
PHY	<i>Physical</i>
PLCP	<i>Physical Layer Convergence Procedure</i>
PMD	<i>Physical Medium Dependent</i>
P/S	<i>Parallel-to-Serial</i>
QAM	<i>Quadrature Amplitude Modulation</i>
QoS	<i>Quality of Service</i>
RS	<i>Random Selection</i>
RTS	<i>Request to Send</i>
SIFS	<i>Short Inteframe Space</i>
SNR	<i>Signal-to-Noise Ratio</i>

Acronyms

S/P	<i>Serial-to-Parallel</i>
SS	<i>Subscriber</i>
STA	<i>Station</i>
UNII	<i>Unlicensed National Information Infrastructure</i>
Wi-Fi	<i>Wireless Fidelity</i>
WLAN	<i>Wireless Local Area Network</i>

Chapter 1

Introduction

1.1 Research Motivations

Quality of Service (QoS) guarantees is becoming increasingly important nowadays since the wireless systems is moving toward the ubiquitous way with high quality wireless services requirements. Supporting various applications, such as file, voice, multimedia and so forth, is one of the critical roles for wireless communications and obviously, different applications require different QoS. Considering the scarcity of the wireless communication resources, i.e. the limited bandwidth and power, it is a great challenge to fulfill the QoS guarantee requirements in wireless communications and lots of issues left unsolved in this area.

In general, wireless communications include concepts and technologies for innovations in architectures, spectrum allocation, and utilization, in radio communications, networks, and services and applications [1]. Therefore, the issue of QoS provision in wireless communications could be addressed from the above aspects.

In this thesis, in order to provide QoS in modern wireless communication systems, we focus on the provision of QoS from different aspects. Firstly, a new system architecture with multiple queues at MAC layer is modeled by a finite state Markov chain to provide diverse QoS in wireless communications. Then, we consider the subcarrier allocation in MU-OFDM system from a cross-layer point of view, with diverse QoS constraints at MAC

layer. Moreover, we also research on the widely investigated IEEE 802.11 WLANs and discuss the channel assignment in this system, oriented by users' QoS requirements.

1.2 Research Objectives

Various algorithms have been proposed in the literature to discuss the QoS guarantee problems in different wireless communication systems. The objective of this thesis is to resolve the problem of QoS provision from different perspectives regarding to different communication systems.

First, since different applications call for different QoS support, providing diverse QoS for different users is essential and imperative in modern wireless communications. With regard to this, the first research objective of this thesis is to extend the conventional single queue finite state Markov chain system model to multiple queues' scenario, such that different users can be provided with different QoS thanks to the diversity introduced by the multiple queues.

Then, most of the existing resource allocation algorithms in MU-OFDM systems are only based on the physical layer information for best-effort performance provision, without any QoS guarantee. Therefore, constrained by users' QoS requirements, we aim at developing a cross-layer subcarrier allocation algorithm which combines the QoS constraints together with the physical layer channel condition to allocate the subcarrier in a manner that users' QoS requirements can be satisfied.

Lastly, we address the issue of channel assignment in IEEE 802.11 WLANs for the sake of solving the problem of frequency scarcity and users' QoS maintainence. In this thesis, we estimate the number of users at physical layer to reduce the latency and when conducting the channel assignment, partially overlapped channels are examined to provide

additional frequency resources and the system QoS performance is the trigger of the channel assignment process.

1.3 Thesis Contributions

The main contributions of this thesis can be summarized as:

- We extend the conventional single queue finite state Markov chain system model to multiple queues' scenario and a priority-based rate allocation algorithm is proposed to explore the diversity of the multiple queues and thus, provide the diverse QoS.
- A cross-layer subcarrier allocation algorithm is proposed in MU-OFDM system, with the diverse QoS constraints at MAC layer. Finite state Markov chain is employed to model the queue status, using which the MAC layer diverse QoS constraints are transformed to the minimum physical layer data rate requirement of each user, which is satisfied through the proposed subcarrier allocation algorithm at physical layer.
- We propose a CIR-based user number estimation algorithm to determine the number of users in IEEE 802.11 channels. The CIR estimation noise is mitigated through an adaptive noise elimination thresholds and when differentiating the CIRs, adaptive CIR determination threshold are introduced to further improve the estimation accuracy.
- A QoS-oriented channel assignment algorithm in IEEE 802.11 WLANs is proposed, where the partially overlapped IEEE 802.11 channels are utilized to solve the problem of frequency scarcity. Moreover, interferences between the partially overlapped channels are mathematically analyzed and involved in the channel assignment.

1.4 Thesis Organization

The rest of the thesis is organized as follows:

Chapter 2 provides the previews of some basic concepts. The discrete-time Markov chain is firstly introduced from a mathematical point of view, followed by the details of queueing system. We then review the OFDM system and the IEEE 802.11 WLAN.

Chapter 3 describes the proposed finite state Markov chain system model with multiple MAC layer queues, where we first briefly introduce the research background and some of the existing related works, followed by the introduction of system model, adaptive modulation and coding (AMC) and physical layer FSMC channel model. The proposed multiple queue finite state Markov Chain system model is then explained in detail, based on which the system QoS performance is analyzed. To evaluate the proposed system, simulation results are presented in the last part of this chapter.

In Chapter 4, we study the subcarrier allocation problem in MU-OFDM system. The MU-OFDM system and the subcarrier allocation problem formulation are first presented, followed by the detailed introduction of the proposed dynamic subcarrier allocation algorithm in a cross-layer way, the MAC layer queue status model and the dynamic subcarrier allocation algorithm at physical layer. Finally, the proposed algorithm is verified through simulations.

The proposed QoS-oriented channel assignment scheme in IEEE 802.11 WLANs with CIR-based user number estimation at physical layer is presented in Chapter 5. Firstly, the estimation of the user number in IEEE 802.11 channels is introduced, including the physical layer model, the mitigation of CIR estimation noise, the derivation of the adaptive CIR determination threshold and the implementation procedure. Then, based on the number of users in each IEEE 802.11 channel, the channel assignment algorithm is explained, where we first mathematically analyze the interferences between the partially overlapped

channels, following which, the channel assignment problem is formulated. After calculating the interference factor (I-factor), we present the details of how the algorithm is implemented. In addition, simulation results are provided to validate both the user number estimation scheme and the channel assignment algorithm.

Finally, Chapter 6 concludes this thesis and suggests some future work.

Chapter 2

Basic Concepts Preview

2.1 Discrete-time Markov Chains

2.1.1 Definition

A discrete-time Markov chain is defined as a stochastic sequence $\{X_k, k \in T\}$ which satisfies the following mathematical condition for $\forall i, \forall j$ and $\forall k$, that is [2]

$$P[X_{k+1} = j | X_0 = i_0, X_1 = i_1, \dots, X_{k-1} = i_{k-1}, X_k = i] = P[X_{k+1} = j | X_k = i], \quad (2.1)$$

where the future probability of the chain only depends on its current state and has no relation with how the chain has arrived. Discrete-time Markov chain is said to be memoryless, because its past history has been completely summarized in current state.

2.1.2 State Transition Probability Formulation

The conditional probability in (2.1) indicates the probability of the chain transiting from state i at time step k to state j at next time step, called as the (one-step) transitional probability. If transitional probability is invariant with respect to the time epoch, we call the chain as *time-homogeneous* Markov chain. Therefore, when representing the transitional probability of a Markov chain, the time step index k can be removed for simplicity and (2.1) is shortly re-written as $p_{ij} = P[X_{k+1} = j | X_k = i]$. In this thesis, all the considered

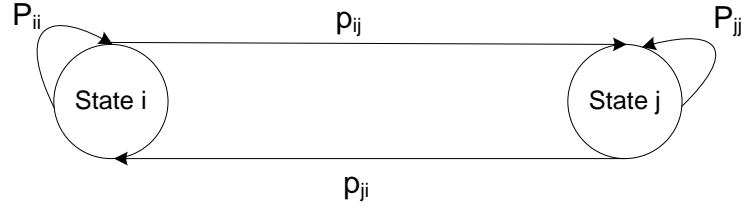


Figure 2.1: State transition diagram of discrete-time Markov chain.

Markov chains are assumed to be time homogeneous, which can most accurately characterize wireless communication systems.

Fig. 2.1 shows that a Markov chain moves from one state i to another state j , called as the system transition whose probability is denoted by p_{ij} . In general, for n states discrete-time Markov chain, we can describe all its transition probabilities through the $n \times n$ transition matrix P_{tran} as

$$P_{tran} = (p_{ij}) = \begin{pmatrix} p_{11} & p_{12} & \cdots & p_{1n} \\ p_{21} & p_{22} & \cdots & p_{2n} \\ \vdots & \vdots & \ddots & \vdots \\ p_{n1} & p_{n2} & \cdots & p_{nn} \end{pmatrix}, \quad (2.2)$$

where due to the fact that system must transit to another state or remain its current state at next time step, P_{tran} is constrained by

$$\sum_j p_{ij} = 1, \forall i. \quad (2.3)$$

2.1.3 State Probability Formulation

When $X_k = i$, we say that the chain is in state i at discrete time step k and the probability of finding the chain in this state is defined as

$$\pi_i^k = P[X_k = i]. \quad (2.4)$$

Using the state transitional probability, we can calculate the probability of finding the chain in a particular state at next time step by

$$\begin{aligned} P[X_{k+1} = j] &= \sum_{i=1}^n P[X_{k+1} = j | X_k = i] \\ &= \sum_{i=1}^n \pi_i^k p_{ij}. \end{aligned} \quad (2.5)$$

Judging from above, it is obvious that a discrete-time Markov chain can be completely characterized by its transition probability matrix in (2.2), given the initial state probability vector π^0 , where we define the state probabilities at time step k as a row vector

$$\pi^k = (\pi_1^k, \dots, \pi_n^k), \quad (2.6)$$

and π^k can be calculated as

$$\pi^k = \pi^{(k-1)} P_{tran} = \pi^{(k-2)} P_{tran}^2 = \dots = \pi^0 P_{tran}^k, \quad (2.7)$$

where P_{tran}^k denotes the k -step transition matrix and P_{tran}^0 is set to be I .

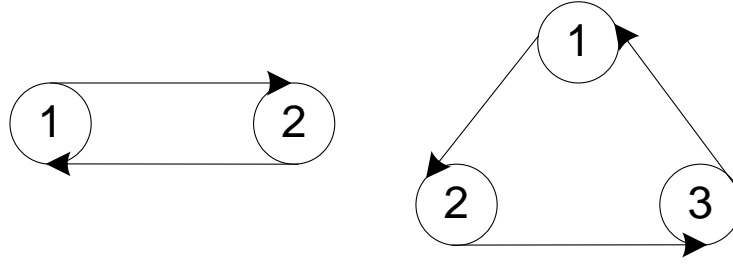


Figure 2.2: Periodic Markov chain.

2.1.4 Steady-state Behavior

2.1.4.1 Ergodic Markov chain

A discrete-time Markov chain is called as *ergodic* if it is *irreducible*, *aperiodic* and *time-homogeneous*, where time-homogeneous Markov chain has been discussed in previous Section and irreducible Markov chain is the one which has only one closed set and all states in the chain can be reached from any other states. Mathematically, it indicates that there exist a $k, k \in [1, +\infty)$, such that $p_{ij}^k > 0, \forall i, j$.

A Markov chain is said to be periodic if it only returns to a particular state after $n\tau, (n = 1, 2, \dots)$ steps with τ the period. Otherwise, we call the Markov chain aperiodic. Fig. 2.2 shows an example of the periodic Markov chain.

2.1.4.2 Stationary distribution of Markov chain

Let $k \rightarrow \infty$ for π^k and P_{tran}^k , we have the steady characteristic of the Markov chain as $P = \lim_{k \rightarrow +\infty} P_{tran}^k$ and $\pi = \lim_{k \rightarrow +\infty} \pi^k$ respectively, which are independent of time step index k . With regard to this, we call the Markov chain has steady state and π is the stationary distribution, calculated by

$$\pi = \pi P. \quad (2.8)$$

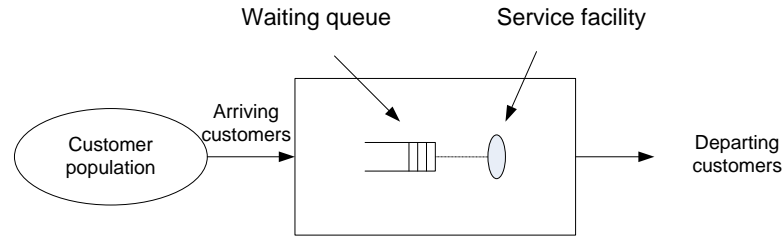


Figure 2.3: Schematic diagram of a queueing system.

According to the theorem in [2], every ergodic Markov chain does exist the stationary distribution which is uniquely determined through the following equations:

$$\pi = \pi P, \quad (2.9)$$

$$\pi \cdot e = 1, \quad (2.10)$$

where e denotes the $1 \times n$ row vector with all the entries equaling to one.

2.2 Queueing System

As depicted in Fig. 2.3, a queueing system is a place where customers arrive according to an arrival process to obtain service from the service facility. Typically, a queueing system is comprised of three major components: the input process, the system structure and the output process.

2.2.1 Input Process

The input process of a queueing system can be characterized by following aspects:

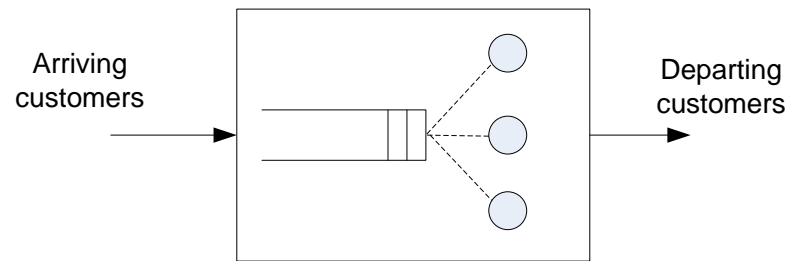


Figure 2.4: System structure of a queueing system: parallel servers.

- The size of arriving population: It may be assumed as either infinite or finite, where for infinite arriving population, the number of external customers is very large compared to that in the system and thus, the arrival rate will not be affected by the size. On the other hand, finite customer population size is more involved because the arrival process is affected by the number of customers which already exist in the system.
- Arriving patterns: This presents how the customers arrive at a queueing system and can be determined by the inter-arrival time between two customers. In practice, a probability distribution is fitted to characterize the time interval where the most frequently adopted distribution in wireless communications is known as Markovian (or Memoryless), which implies Poisson process.
- Behavior of arriving customers: The customers which arrive at a full queue due to the finite length of the queue may either leave forever without entering the system, called blocking system or come back after a short while.

2.2.2 System Structure

The service facility in Fig. 2.3 consists of one or more servers, categorized into the parallel servers and the serial servers, shown in Fig. 2.4 and Fig. 2.5 respectively. In parallel servers, the customer at the head of the waiting queue can go to any server which is avail-

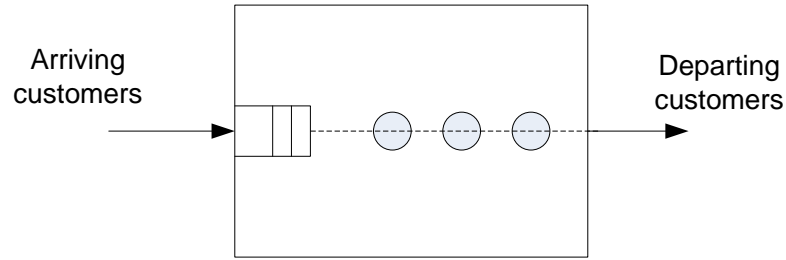


Figure 2.5: System structure of a queueing system: serial servers.

able for serving and leave the system after receiving the service, while for the serial servers, the customer receives services from all or some of serial services before it leaves the systems. In this thesis, considering the practical situation in wireless communications, only the parallel servers are investigated.

Another important characteristic to describe the system structure is the system capacity, referring to the maximum number of customers that the queueing system can deal with, inclusive of those customers at the service facility. Specifically, in the parallel server queueing systems, the system capacity is obtained by summing the maximum size of the waiting queue and the number of servers.

2.2.3 Output Process

In general, there are five disciplines, which determine how the customers are selected for services, those are first-come-first served (FCFS), last-come-first-served (LCFS), priority, processor sharing and random. Among these disciplines, FCFS (also known as FIFO, standing for first-in-first-out) is commonly adopted in wireless communications for the ordered queue.

Similar to the arrival patterns, as every customer requires different amounts of service times, a probability distribution could be used to describe the length of service times to the customers, where negative exponential distribution is the usually encountered one.

2.2.4 Kendall Notation

To categorize and describe the different kinds of queueing systems, David G Kendall firstly devised a shorthand notation with only single waiting queue considered in 1953. This notation is known as Kendall notation, as follows [2]:

$$A/B/X/Y/Z$$

- A: Customer arriving pattern
- B: Service pattern
- X: Number of parallel servers
- Y: System capacity
- Z: Queueing discipline.

Taking $M/M/1/\infty/FCFS$ as an example, it can be explained as a queueing system where customers arrival is modeled by Poisson process and the exponentially distributed service times from the server are requested. Moreover, the system has only one server, an infinite queue length and the customers are served on a FCFS basis. For simplicity, in practice, only the first three parameter are presented and by default, the last two parameters are assigned with $Y = \infty$ and $Z = FCFS$ respectively.

2.3 OFDM System

2.3.1 Concept of OFDM

OFDM which stands for orthogonal frequency division multiplexing, was firstly introduced in 1970s by S. Weinstein and P. Ebert [4]. By dividing the wider band frequency selective

channels into a set of narrow band flat fading subchannels, the influences of inter-symbol interferences (ISI) could be eliminated.

The time domain OFDM symbol can be expressed as

$$x(t) = \sum_{k=0}^{N-1} X(k)e^{j2\pi f_k t}, \quad 0 \leq t < T_s, \quad (2.11)$$

where $X(k)$ denotes the data transmitted on the k -th subcarrier, N is the number of subcarriers in the OFDM symbol and T_s is the symbol duration. As for f_k , it is the frequency of the k -th subcarrier, given by $f_k = f_0 + k\Delta f$, where Δf is the subcarrier spacing, constrained by the orthogonality condition in order to demodulate the OFDM signal for the receiver, that is $T_s\Delta f = 1$.

Thanks to the orthogonal condition, it is evident that all the subcarriers are orthogonal to each other, which can be easily demonstrated as follows [5]:

$$\begin{aligned} & \frac{1}{T_s} \int_0^{T_s} e^{j2\pi f_k t} (e^{j2\pi f_l t})^* dt \\ &= \frac{1}{T_s} \int_0^{T_s} e^{j2\pi(f_k - f_l)t} dt \\ &= \frac{1}{T_s} \int_0^{T_s} e^{j2\pi(k-l)\Delta f t} dt \\ &= \delta[k - l], \end{aligned} \quad (2.12)$$

where $\delta[k - l]$ denotes the delta function, defined as [6]

$$\delta[k - l] = \begin{cases} 1, & k = l, \\ 0, & \text{otherwise.} \end{cases} \quad (2.13)$$

Assuming the system samples $x(t)$ at the interval of $T_{sa} = \frac{T_s}{N}$, the sampled symbol can be obtained as

$$x(n) = \sum_{k=0}^{N-1} X(k)e^{j2\pi f_k \frac{nT}{N}}, \quad n = 0, 1, 2, \dots, N-1. \quad (2.14)$$

Without loss of generality, let $f_0 = 0$. Therefore,

$$f_k T_s = T_s(f_0 + k\delta f)T_s = kT_s\delta f = k, \quad (2.15)$$

and (2.12) becomes

$$x(n) = \sum_{k=0}^{N-1} X(k)e^{jf_k \frac{2\pi kn}{N}} = \text{IDFT}(X(k)), \quad (2.16)$$

where IDFT is the abbreviation of inverse discrete Fourier transform, indicating that OFDM modulation can be easily implemented using IDFT. In reality, inverse fast Fourier transform (IFFT) which can reduce the number of complex multiplications from N^2 to $\frac{N}{2} \log_2 N$ for an N -point IDFT, is adopted for more efficient implementation of the OFDM system.

Furthermore, in order to eliminate the effect of time-dispersive multipath channel, known as the intersymbol interference (ISI), a cyclic prefix (CP) whose length is required to exceed the maximum excess delay of the multipath propagation channel is employed in each OFDM symbol. A CP is typically a copy of the last part of one OFDM data symbol and appended at the beginning of that symbol, as illustrated in Fig. 2.6.

2.3.2 OFDM Transmitter

A block diagram of the OFDM transmitter is depicted in Fig. 2.7, and consists of a total of eight blocks, namely channel coding and interleaving, symbol mapping, serial-to-parallel

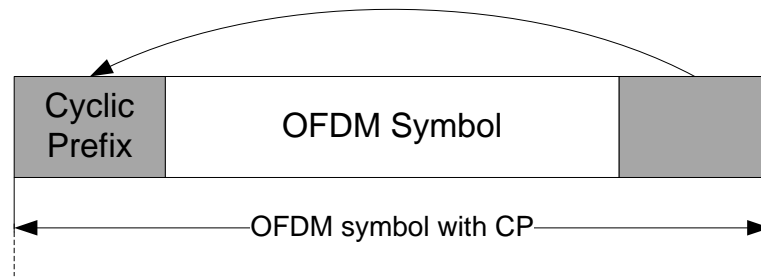


Figure 2.6: The structure of OFDM symbol with cyclic prefix.

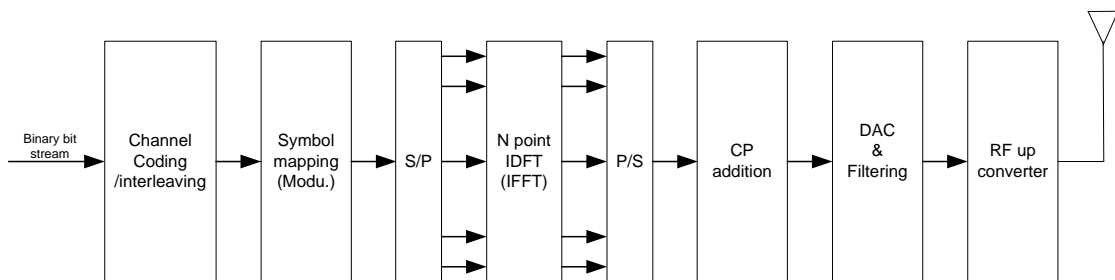


Figure 2.7: Block diagram of OFDM transmitter.

(S/P) conversion, IFFT, parallel-to-serial (P/S) conversion, CP addition, digital-to-analog conversion (DAC) and RF up conversion.

More specifically, the binary bit stream, which refers to the information to be transmitted over the wireless channels, is first coded and interleaved for better bit-error-rate (BER) performance, where the channel coding provides the ability of error detection and correction while interleaving reduces the impact of burst errors. Next, the symbol mapping block converts the coded and interleaved bit stream into the symbol stream as shown in Fig. 2.8 where 16-QAM (Quadrature Amplitude Modulation) is given as an example. After that, the symbol stream is re-organized via the serial to parallel conversion and then modulated by IFFT where the pilots are inserted at this stage for channel synchronization and estimation at the receiver. Following the P/S conversion, additional symbols are appended and the appended symbol is then converted into an analog signal by the digital-to-analog converter (DAC). Finally, the analog signal is subject to a low-pass filter, up-converted to the desired

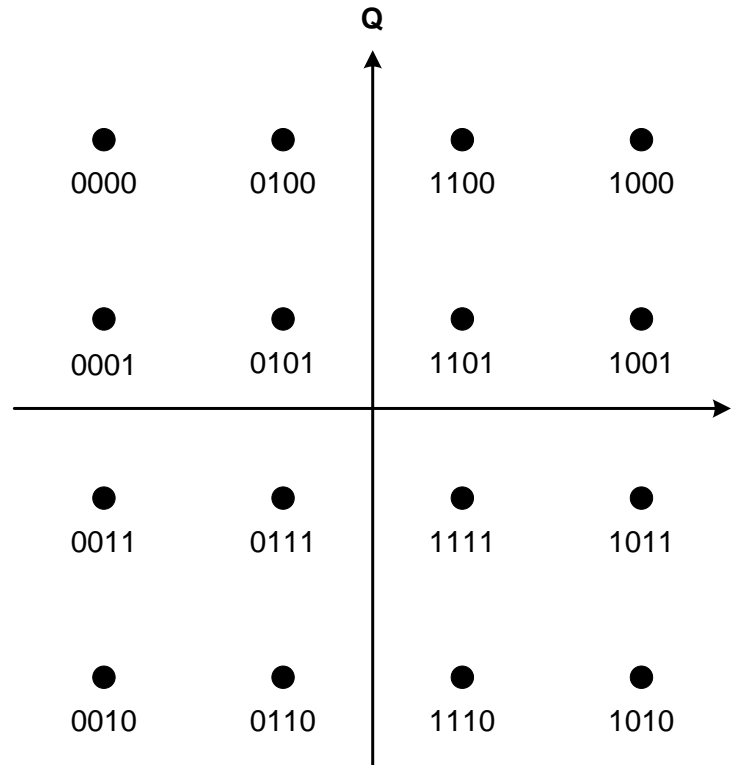


Figure 2.8: Constellation diagram for rectangular 16-QAM.

frequency and amplified before transmitted via the antenna.

2.3.3 OFDM Receiver

Fig. 2.9 shows the system blocks of the OFDM receiver where most blocks perform the reverse functions of the transmitter. To be more specific, the received signal is first subject to a band-pass filter and then down-converted to baseband signal, which is sampled by the analog-to-digital converter (ADC). After synchronizing in both time and frequency domain, CP is removed and the operated symbol is later processed by fast Fourier transform (FFT) with the channel distortion compensated. At the final stage, the signal is demodulated, de-interleaved and decoded to recover the transmitted information.

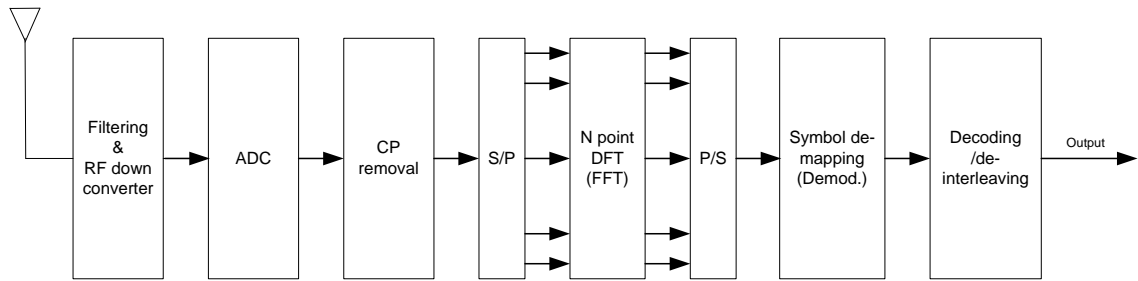


Figure 2.9: Block diagram of OFDM receiver.

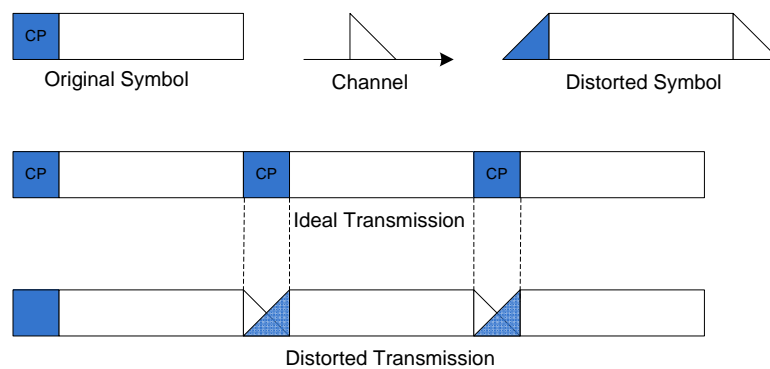


Figure 2.10: Elimination of ISI through cyclic prefix.

2.3.4 Advantages and Disadvantages of OFDM systems

The reason why OFDM is being widely deployed in modern systems and standards is that it can significantly improve the performance of broadband wireless communications due to the following advantages that it can achieve:

- **Immunity to multipath fading:** Given the length of the CP is larger than the maximum excess delay of the multipath propagation channel, it is demonstrated in Fig. 2.10 that the multipath interference from the preceding symbol can be absorbed by the CP of current symbol. Therefore, by removing the CP before OFDM symbol demodulation, the ISI is eliminated.
- **Spectral efficiency:** As show in Fig. 2.11, because of the orthogonal subcarriers which have been most tightly packed, OFDM systems can further improve the fre-

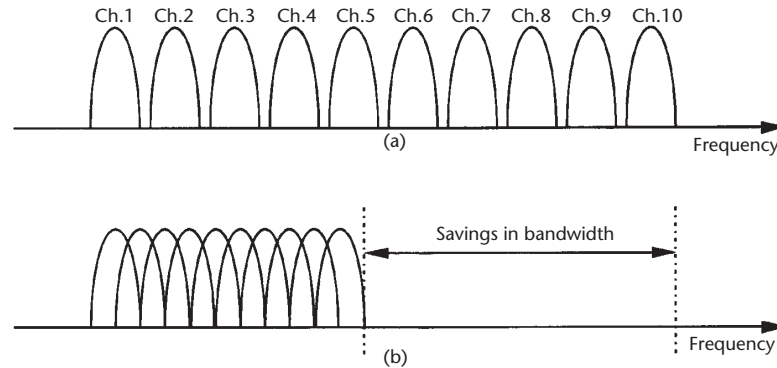


Figure 2.11: Bandwidth utilization comparison between the OFDM system and the conventional FDM system [7].

quency efficiency compared to the conventional FDM systems. Moreover, it eliminates the inter-carrier interference (ICI) and leads to easier signal separation at the receiver.

Besides, OFDM systems also have the benefits of flexible in resource allocation, noise immunity, easy to integrated with other techniques and so forth [8]. However, on the other hand, OFDM also has its drawbacks where the major issues are:

- High peak-to-average power ratio (PAPR): OFDM signals are the summation of all the OFDM subcarriers, unavoidably resulting in the high PAPR which correspondingly, requires large linear range of the DAC and power amplifier to avoid severe clipping and non-linear distortion. This increases not only the power consumptions, but also the complexity of the system implementation.
- Sensitivity to frequency offset and phase noise: OFDM systems can tolerate the time offset because of the use of cyclic prefix which extends the symbol in time domain. However, they could be very sensitive to the carrier frequency offset (CFO) and phase noise, which may lead to the loss of orthogonality between subsymbols and thus, dramatically degrade the system performance [9].

- Capacity and power loss: Due to the transmission of the CP in OFDM symbols, extra frequency resource and power have to be spent on those effectiveness symbols, reducing the system capacity and power efficiency.

2.4 IEEE 802.11 WLAN

2.4.1 Overview of WLAN

A wireless local area network (WLAN) is a wireless communication system that uses radio waves as the transmission media [10] to link the computers or workstations, and provides a connection to the internet through an access point (AP). In recent years, WLAN is experiencing tremendous growth and becoming increasingly popular, due to the efficiently join data connectivity and mobility within a limited geographical area. A typical WLAN consists of a wireless network interface card, known as station (STA), and a wireless bridge referred to as an AP, which connects the wireless network to the wired network (e.g., Ethernet LAN).

There are two main standards used in WLANs, namely the high performance radio local area network (HiperLAN), proposed by European Telecommunications Standards Institute (ETSI) [11], and the 802.11 standard proposed by IEEE [12], among which the IEEE 802.11 standard is employed in most of the existing WLAN systems, also known as Wi-Fi (wireless fidelity). IEEE 802.11 provides the regulations on designing the physical (PHY) layer and the medium access control (MAC) layer for different vendors to operate in systematic way over the wireless radio frequency bands.

2.4.2 The PHY and MAC of WLAN

2.4.2.1 The physical layer

The physical layer of IEEE 802.11 WLAN is composed of two components: the Physical Layer Convergence Procedure (PLCP) and the Physical Medium Dependent (PMD) layer, where PLCP simplifies the provision of a physical service interface to the IEEE 802.11 MAC services while PMD provides a transmission interface used to send and receive data between two or more STAs [12].

Three types of physical techniques are defined for WLAN, those are infrared light (IR), frequency hopping spread spectrum (FHSS) and direct sequence spread spectrum (DSSS), where IR works at the baseband and the other two operate at the licence-free 2.4GHz Industrial, Scientific, and Medical (ISM) band or the higher 5GHz Unlicensed National Information Infrastructure (U-NII) band. Recently, due to the requirement for high data rate, multiple-input multiple-output (MIMO) is taken into consideration in the new IEEE 802.11n standard, which takes advantage of the multi-path environments, leading to a potential capacity increment. The below lists some examples of the physical layer in some of the current standards [13]:

- a. High-Rate Direct Sequence (HR/DS or HR/DSSS) used in 802.11b
- b. Orthogonal Frequency Division Multiplexing (OFDM) used in 802.11a
- c. Extended Rate PHY (ERP) used in 802.11g
- d. MIMO used in 802.11n

2.4.2.2 The media access control layer

IEEE 802.11 MAC architecture can be described as shown in Fig. 2.12 as providing the PCF (point coordination function) through the services of the DCF (distributed coordination function). DCF is the fundamental access method of IEEE 802.11 MAC and required

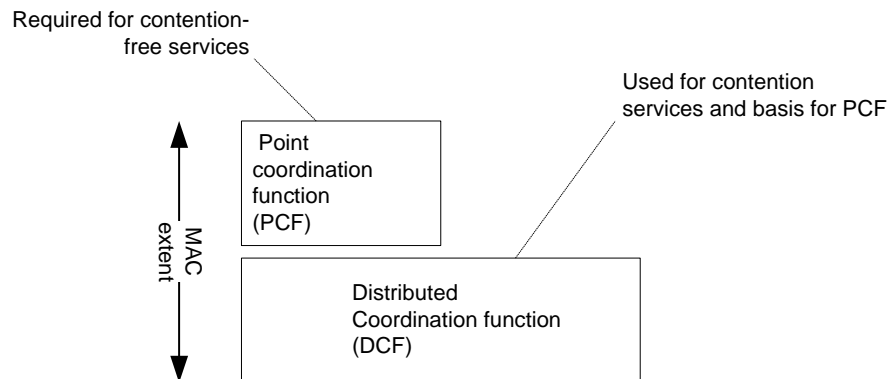


Figure 2.12: IEEE 802.11 MAC architecture.

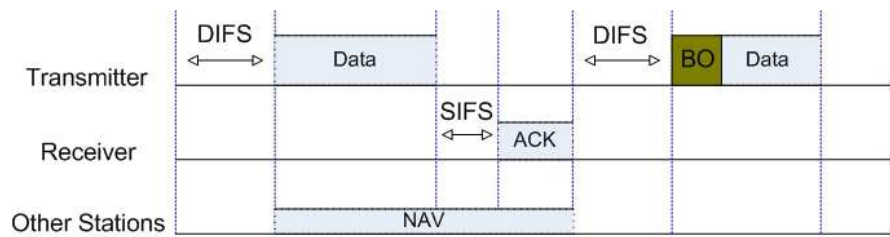


Figure 2.13: CSMA/CA basic access mechanism.

to be supported by all the STAs as defined in IEEE 802.11 specifications [14]. It is known as carrier sense multiple access with collision avoidance (CSMA/CA) where the STA with packets to transmit must contend for access to the channel. On the other hand, PCF uses a point coordinator (PC) working at the access point to determine which STA currently has the priority to transmit and provides the contention-free service as well as the QoS to some real-time applications. In this section, we focus on detailing the DCF, while the details of PCF can be found in [15, 16, 17].

To implement the DCF, two access mechanisms and two types of carrier-sensing mechanisms are defined respectively, i.e basic access and request to send/clear to send (RTS/CTS) access mechanisms, and physical carrier-sensing performed at air interface and virtual carrier-sensing performed at the MAC sublayer. For the basic access model, when the STA requires to transmit, if the channel is sensed busy, the STA has to wait until the

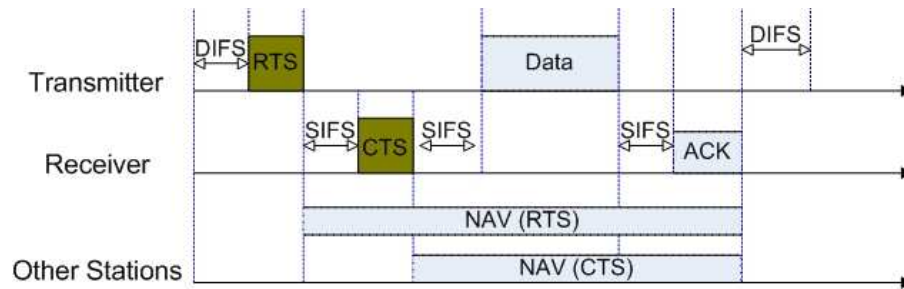


Figure 2.14: CSMA/CA CTS/RTS mechanism.

channel becomes idle for a distributed interframe space (DIFS) period and then starts a random backoff timer. The backoff time is set as a uniformly random number from the interval $[0, CW-1]$, where CW denotes the contention window size. For each unsuccessful transmission, the value of CW is doubled until reaching a maximum value CW_{max} or it is set to a minimum value CW_{min} when the frame is either dropped or successfully transmitted. The STA decrements the backoff timer by one if the medium becomes idle for a DIFS period, otherwise it freezes the timer. Upon the timer is decremented to zero, the STA transmits its frame and an acknowledgement (ACK) will be reported by the receiver after a short interframe space (SIFS) period of successfully receiving the packet. However, if the ACK is missed caused by two or more STAs decrementing to zero simultaneously, the STA will retransmit the frame with the increased CW size. The CSMA/CA basic access mechanism is shown in Fig. 2.13.

For the sake of resolving the problem of hidden terminal in IEEE 802.11 WLANs, which refers to the nodes within the interference range of the intended destination and out of the carrier sensing range of the source [18, 19], an optional four way hand-shaking technique, known as the CSMA/CA RTS/CTS mechanism is introduced, shown in Fig. 2.14. Before a STA attempts to transmit a frame, it sends a short RTS frame, and the receiver replies with a CTS frame to indicate whether it is ready to receive. Once the transmitter receives the CTS frame, it starts the transmission. Other STAs hearing the

RTS update their network allocation vector (NAV) with the duration of the data frame transmission.

2.5 Summary

In this chapter, we have reviewed some basic concepts to provide a basis for the rest of this thesis. Firstly, the finite-state Markov chain which could be used to model the wireless channels as well as the communication system was presented from the mathematics point of view, followed by the introduction of the queueing system which is being broadly involved in MAC layer queue status modeling. Then, two typical systems, namely the OFDM and WLANs, based on which the works in this thesis are carried out, have been explained in detail.

Chapter 3

Modeling of Wireless Communications for Diverse QoS Provision

In wireless communications, it is necessary and challenging to guarantee diverse quality of service (QoS) for various applications over wireless fading channels. In this chapter, using the cross-layer approach [20], a finite state Markov chain system model with multiple queues deployed at MAC layer is proposed to address the issue of diverse QoS provision in wireless communications. We first model the physical (PHY) layer channel by finite state Markov channel (FSMC) and then, combine FSMC with the queue status at MAC layer to construct the finite state Markov chain model for the communication system. To guarantee different queues with different priorities and provide the diverse QoS, a *priority-based rate allocation algorithm*, named as PRA algorithm, is introduced to distribute the physical layer data rate to the multiple MAC layer queues, where higher priority queue can obtain larger data rate for transmission and vice versus, leading to diverse QoS provision in the proposed system.

3.1 Introduction

One notable feature in nowadays wireless communications is the requirement of diverse quality of service (QoS) provision, due to the various of applications, such as video/audio, file etc. Providing diverse QoS, in terms of packet error/loss rate and average system delay,

to different users is regarded to be a challenge because of the scarcity of wireless resources (bandwidth and power), multipath fading channels and Doppler effects. Therefore, the researches on guaranteeing QoS in wireless communications have drawn many researchers' attentions recently [21, 22, 23, 24].

Facing the dramatic variation nature of wireless link, caused by Doppler effect and multipath fading, it has been widely recognized to use finite-state Markov channel (FSMC) to model such time-varying wireless fading channels, firstly proposed in [25]. FSMC partitions the received signal to noise ratio (SNR) into a finite number of intervals with each interval representing a state of a Markov process [25, 26, 27]. Moreover, adaptive modulation and coding (AMC) is usually adopted to match the partitioned channel states by changing the transmission parameters at the transmitter, bringing the benefits of attractive rate and error performance [28, 29].

Using the cross-layer design approach, in [29], Liu et al. firstly combined the FSMC channel at physical layer with the single queue at MAC layer to construct a new finite-state Markov chain system model, for the sake of analyzing the long-time transmission system performance. Originating from this work, lots of other subsequent researches have been conducted to improve the wireless communication performance, such as the energy-efficient wireless communications proposed in [30, 31]. Motivated by addressing the QoS problems mentioned above, authors in [32, 33] used the MAC layer scheduling mechanism to provide diverse QoS for different users, where different connections were assigned different priorities and higher priority connection was scheduled earlier for better QoS.

However, most of the previous works using physical layer FSMC only assume single MAC layer queue while employing multiple queues can introduce diversity to the communication systems and most importantly, bring the convenience of providing diverse QoS for different applications. Therefore, we extend the work in [29] to a more general scenario, that is multiple queues are assumed to be deployed at MAC layer in our proposed model,

and using the cross-layer technique, we use a finite state Markov chain to model the communication system by combining the queues' status at MAC layer with the FSMC channel states at physical layer. Firstly, the physical layer slow-fading channel is modeled by a finite state Markov channel (FSMC) and adaptive modulation and coding is adopted corresponding to the channel states for the stable physical layer performance, i.e. a constant packet error rate (PER) at physical layer. At MAC layer, the queues are considered to be finite length and different queues handle the data with different QoS requirements. To differentiate the multiple queues, a priority-based rate allocation algorithm is introduced, where we assume that the physical layer transmission rate is allocated to the multiple queues proportionally with the queue containing higher QoS requirement data obtaining larger data rate. As a result, diverse QoS is provided to the multiple queues. Finally, deriving from the multiple queue status at MAC layer, the channel state at physical layer and the proposed PRA algorithm, a multiple dimensional finite state Markov chain is constructed to model the communication system, and its QoS performance is analyzed and simulated to verify the diverse QoS provision in the proposed system.

3.2 System Model

3.2.1 System Description

Fig. 3.1 shows a basic wireless communication systems, where multiple subscribers (SS) are connected to the base station (BS) over the time-varying wireless channels. For different users, they may transmit different kinds of data and thus require different QoS guarantee. For instance, real time data such as voice and video, is more delay-sensitive while in the mean time, some other kinds of data, such as file-based data requires zero-error tolerance transmission and can however bear longer system latency.

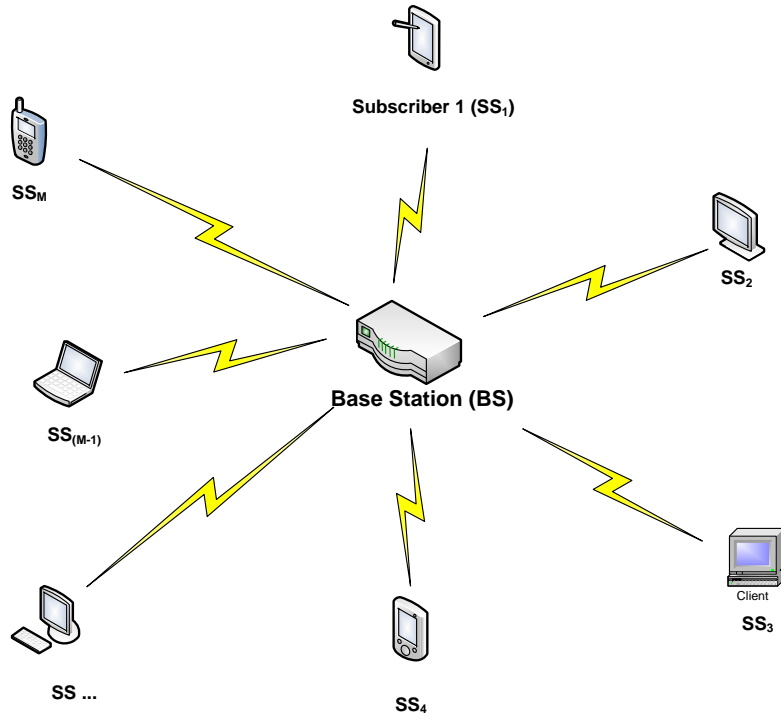


Figure 3.1: Wireless communication system diagram with a base station associated by multiple subscribers

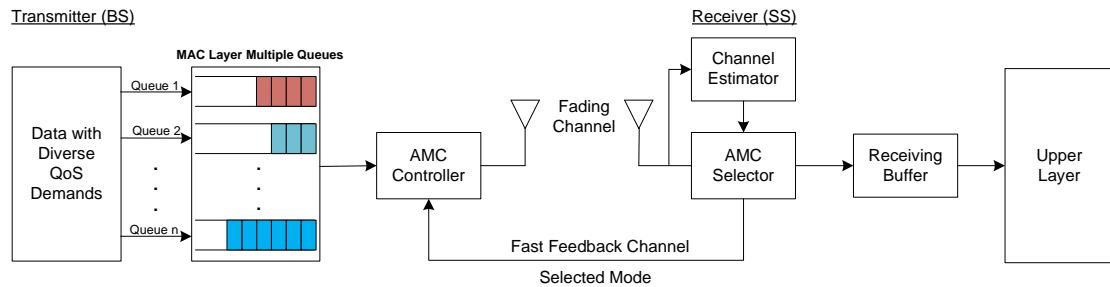


Figure 3.2: Wireless link from the base station (BS) to a subscriber (SS)

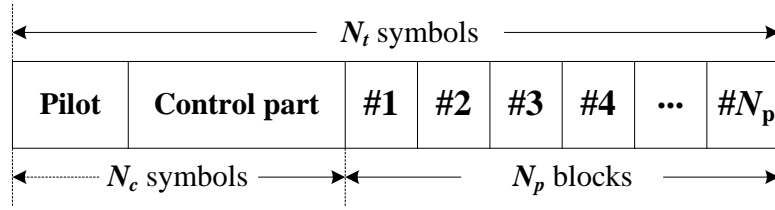


Figure 3.3: Physical layer frame structure

As for the wireless link between the BS and a SS, it is simply considered as shown in Fig. 3.2, where M MAC layer queues are employed at the base station, and packets with similar QoS requirements are grouped in the same queue while packets with different QoS requirements are in different queues. The data from the multiple queues are then handled by the AMC controller and transmitted using certain transmission mode according to the feedback from the receiver. At the receiver side, AMC selector is introduced to determine the suitable modulation and coding scheme based on the estimated channel state information (CSI). The decision of AMC selector is then reported to the AMC controller at the transmitter through a fast feedback channel to update the transmission mode.

For the physical layer, we consider that it operates on a frame by frame basis where each frame has a fixed time duration (T_f) and consists of a fixed number of symbols (N_t). The frame structure is shown in Fig. 3.3, where symbols transmitted during each time frame are grouped into two sections according to their applications, i.e. frame control section with N_c symbols and data transmission section with N_d symbols. The frame control section can be further divided into two parts, the pilot and the control part. The pilot is transmitted with constant power and allows the receiver to estimate the instantaneous channel state information while the control part contains the current transmission mode information, used for demodulation and decoding at the receiver side. The data transmission section consists of N_p MAC layer packets where N_p varies and depends on current communication system condition. Using AMC mode k , each packet is modulated and coded with rate R_k (bits/symbol) and then turns into N_b/R_k symbols where N_b is the packet length in *bits*.

Thus, the number of symbols transmitted per frame is obtained as $N_t = N_c + N_d = N_c + N_p N_b / R_k$.

Besides the above descriptions, we next list some other assumptions for the proposed system as follows:

- The queueing system is considered to be a blocking system, as discussed in chapter 2.2.1. To be more specific, the multiple queues at MAC layer are of finite-length with the possibility of buffer overflow and arriving packets will be dropped once the queues are full where the dropped packets will no longer be re-transmitted.
- packets arriving in time frame t ($[tT_f, (t + 1)T_f)$) are enqueued at time slot $(t + 1)T_f$ and will be served in time frame $t + 1$.
- The wireless channel is modeled as slowly varying flat-fading channel and remains constant for one time frame. However, the change of wireless channel between time frames is allowed.
- Perfect channel state information estimated at the receiver side is available for both the transmitter and the receiver.
- Multiple transmission modes are available with each mode, a combination of specific modulation scheme and a forward error correcting (FEC) code. Details of the available transmission modes will be covered later.

3.2.2 Adaptive Modulation and Coding

For the purpose of maximizing the data rate, adaptive modulation and coding (AMC) changes the modulation and coding mechanisms at the transmitter according to the variations of the channel condition under the constraints of communication system, where the

Table 3.1: Transmission Modes with Uncoded M_n -QAM Modulation

	Mode 1	Mode 2	Mode 3	Mode 4	Mode 5
Modulation	BPSK	QPSK	8-QAM	16-QAM	32-QAM
R_k (bits/sym.)	1	2	3	4	5
a_k	67.7328	73.8279	58.7332	55.9137	50.0552
g_k	0.9819	0.4945	0.1641	0.0989	0.0381
γ_{pk} (dB)	6.3281	9.3945	13.9470	16.0938	20.1103

Table 3.2: Transmission Modes with Conventionally Coded Modulation

	Mode 1	Mode 2	Mode 3	Mode 4	Mode 5
Modulation	BPSK	QPSK	8-QAM	16-QAM	32-QAM
Coding rate R_c	1/2	1/2	3/4	3/4	3/4
R_k (bits/sym.)	0.5	1	1.5	3	4.5
a_k	274.7229	90.2514	67.6181	53.3987	35.3508
g_k	7.9932	3.4998	1.6883	0.3756	0.0900
γ_{pk} (dB)	-1.5331	1.0942	3.9722	10.2488	15.9784

channel condition is estimated at the receiver and then, reported to the transmitter through a special feedback channel.

Tab. 3.1 and 3.2 present two groups of typical transmission modes for the physical layer, each of which is associated with a specific AMC scheme. In practice, as depicted in Fig. 3.2, the AMC selector at receiver selects a particular mode according to current CSI and report the result to the transmitter to update the transmission mode for next time frame.

The major benefits for AMC are two-fold [34], 1) higher data rate can be achieved due to the rate maximization objective in AMC, which in turn increases the average system throughput; 2) the variation of interference can be reduced since the transmitter changes the modulation/coding scheme rather than adjusting the transmission power, to cope with the channel condition.

On the other hand, the performance of AMC highly relies on the following factors [35, 36]:

- The operational environment: We use the CSI in current time frame to select the

transmission mode for next time frame. In light of this, the AMC can only operate efficiently in an environment where the channel is assumed to be relatively slowly-varying, otherwise the selected modulation/coding scheme may not be fit for the channel condition in next time frame.

- The transmission modes: Ideally, it is better to provide as many transmission modes as possible, such that the channel condition can be most precisely matched. However, the increasing of the available transmission modes increases the system implementation complexity as well. Therefore, there is a tradeoff between the AMC performance and the system complexity, which needs to be carefully examined in the design of AMC systems.
- The feedback mechanism: Since the wireless channels are time-varying, the feedback of the CSI becomes an issue. It is necessary to assume a slowly-varying channel as well as a reliable feedback to guarantee the performance of AMC. In this case, no delay and transmission errors are allowed in the feedback channel to promise there is no discrepancy existing between AMC mode selected at the receiver and mode used for transmission at the transmitter.

3.2.3 Finite State Markov Channel

The modeling of the Rayleigh fading channel [37] using a Markov chain was firstly proposed by Wang and Moayeri in 1995 [25], called as finite State Markov Channel (FSMC), where the received SNR is partitioned into a finite number of non-overlapping consecutive intervals with each interval representing a state of channel. FSMC are mathematically derived from the discrete-time Markov chain as we discussed in Chapter 2.2, where the channel states correspond to the states in a Markov chain.

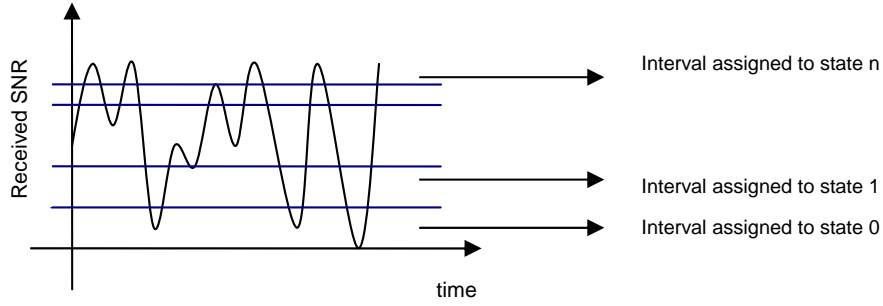


Figure 3.4: Channel partitioning in FSMC [38]

3.2.3.1 Channel partitionings

To construct the finite state Markov channel model, we first partition the channel through partitioning the received SNR into several intervals, as shown in Fig. 3.4. Numerous channel partitioning schemes have been proposed in literatures, such as equal probability partitioning, uniform partitioning, linearly increasing probabilities partitioning and so forth [25, 26, 27, 39], among which the equal probabilities channel partitioning is being widely deployed, where the threshold are selected in such a way that the state probability of being in any state are equal [25].

We assume that the channel is partitioned into $N + 1$ intervals, corresponding to $N + 1$ channel states which are denoted by $S = \{S_0, S_1, \dots, S_N\}$. In order to maintain a prescribed packet error rate P_e at physical layer, adaptive modulation and coding is employed by adjusting the available transmission modes T_m according to the CSI estimated at the receiver, i.e. transmission mode k is adopted when the channel is in state S_k , $k \in [0, N]$.

The noise is assumed to be additive Gaussian noise (AWGN) with received SNR γ , whose probability density function (PDF) follows exponential distribution as

$$p(\gamma) = \frac{1}{\gamma_0} \exp\left(-\frac{\gamma}{\gamma_0}\right), \quad \gamma \geq 0, \quad (3.1)$$

where γ_0 is the average received SNR.

In the presence of AWGN noise, the packet error rate can be approximated as

$$\text{PER}(\gamma) = \begin{cases} 1, & 0 < \gamma < \gamma_{pk} \\ a_k \exp(-g_k \gamma), & \gamma \geq \gamma_{pk}, \end{cases} \quad (3.2)$$

where k is the channel state index and γ is the received SNR. The parameters a_k , g_k and γ_{pk} are obtained by fitting (3.2) to the exact packet error rate.

We assume that the threshold of the partitioned received SNR for each state are denoted as $\Gamma_0 = 0 < \Gamma_1 < \Gamma_2 < \dots < \Gamma_N = \infty$ and the channel is defined in state S_k if the received SNR γ falls in $[\Gamma_k, \Gamma_{k+1})$. Therefore, the steady state probability π_k when the channel is in state S_k can be given by

$$\pi_k = \int_{\Gamma_k}^{\Gamma_{k+1}} p(\gamma) d\gamma, \quad k = 0, 1, \dots, N \quad (3.3)$$

and correspondingly, the average packet error rate for channel state S_k is

$$\overline{\text{PER}(k)} = \frac{1}{\pi_k} \int_{\Gamma_k}^{\Gamma_{k+1}} \text{PER}(\gamma) p(\gamma) d\gamma, \quad k = 0, 1, \dots, N \quad (3.4)$$

Searching-based channel partitioning scheme is adopted in our proposed model, where it searches to find the threshold $\{\Gamma_k\}_{k=0}^{N+1}$ such that the prescribed packet error rate P_e is constant regardless of the channel states, that is $\overline{\text{PER}(k)} = P_e, \forall k$. In this case, we can easily prove as follows that the average packet error rate of the communication system

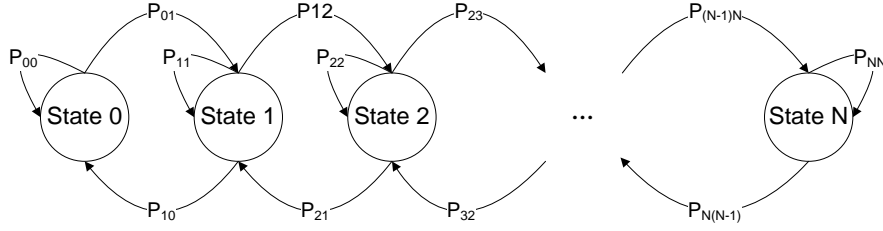


Figure 3.5: N + 1 finite state Markov channel

$\overline{\text{PER}}$ can maintain P_e during the whole transmission time, i.e. $\overline{\text{PER}} \equiv P_e$.

$$\begin{aligned}
 \overline{\text{PER}} &= \sum_{k=0}^N \pi_k \cdot \overline{\text{PER}}(k) \\
 &= P_e \sum_{k=0}^N \pi_k \\
 &= P_e.
 \end{aligned} \tag{3.5}$$

Below shows the detailed procedure of how the SNR thresholds $\{\Gamma_k\}_{k=0}^{M+1}$ is determined using a searching mechanism.

Step a: Set $k = N$, $\Gamma_{k+1} = +\infty$.

Step b: For each k , search for the $\Gamma_k \in [0, \Gamma_{k+1}]$, such that $\overline{\text{PER}}(k) = P_e$.

Step c: If $k > 1$, set $k = k - 1$ and go to Step b; otherwise, go to next step.

Step d: Set $\Gamma_0 = 0$.

3.2.3.2 Channel state transition probabilities

Let $\{S_i\}$, $i = 0, 1, \dots$ be a stationary Markov process, we get the transition probability, independent of time index as

$$P_{s,l} \equiv Pr(S_{i+1} = S_l | S_i = S_s), \quad s, l \in \{0, 1, \dots, N\}. \tag{3.6}$$

As shown in Fig. 3.5, the transition only occurs between two adjacent states with the assumptions of the slow fading channel. Therefore, we have

$$P_{s,l} = 0, \quad \forall |s - l| \geq 2. \quad (3.7)$$

With regard to this, we are only interested in the adjacent-transition probability, given by

$$P_{k,k+1} = \frac{N_{k+1}T_f}{\pi_k}, \quad \text{if } k = 0, 1, \dots, N-1, \quad (3.8)$$

$$P_{k,k-1} = \frac{N_k T_f}{\pi_k}, \quad \text{if } k = 0, 1, \dots, N, \quad (3.9)$$

where N_k is the level crossing rate (LCR) measuring the rapidity of channel fading, calculated by

$$N_k = \sqrt{\frac{2\pi\Gamma_k}{\gamma_0}} f_d \exp\left(-\frac{\Gamma_k}{\gamma_0}\right), \quad (3.10)$$

where f_d denotes the Doppler frequency caused by user mobility. The probability of staying at the same state is

$$P_{k,k} = \begin{cases} 1 - P_{k,k+1} - P_{k,k-1}, & \text{if } 0 < k < N \\ 1 - P_{0,1}, & \text{if } k = 0 \\ 1 - P_{N,N-1}, & \text{if } k = N \end{cases}. \quad (3.11)$$

We can now model the Rayleigh fading channel as $N + 1$ states Markov channel with its $(N + 1) \times (N + 1)$ state transition matrix P_c calculated by combining (3.7) to (3.11).

3.3 Proposed Multiple Queue Finite State Markov Chain System Model

To model the communication system, we combine the FSMC at physical layer with the multiple queues' status at MAC layer to construct a finite state Markov chain. Stationary distribution of the obtained Markov chain is calculated to analyze the diverse system performance, in terms of packet loss rate and average system delay.

3.3.1 Queue Behavior Modeling

We consider the M/M/1/ B_i /FCFS model for Q_i in the proposed system, that is a queueing system where customers arrival is modeled by Poisson process and the exponentially distributed service times from the server are requested. Moreover, the system has only one server, an finite queue length (B_i) and the customers are served on a FCFS basis.

Let A_t^i ($i \in [1, M]$) denote the number of packets arriving at time frame t for Q^i , which is assumed to be Poisson distributed with parameters $\lambda^i T_f$,

$$P(A_t^i = a) = \begin{cases} \frac{(\lambda^i T_f)^a \exp(-\lambda^i T_f)}{a!}, & i = 1, 2, \dots, M \text{ and if } a \geq 0 \\ 0, & \text{otherwise} \end{cases}, \quad (3.12)$$

where $E[A_t^i] = \lambda^i T_f$ with $E[A_t^i] \in A := \{0, 1, \dots, \infty\}$ and $E[\cdot]$ denoting the expectation of a random variable.

We use R_t^i (packets/time frame) to denote the number of packets transmitted at time

frame t for Q^i . Obviously, R_t^i should satisfy the following constraints,

$$\begin{aligned} 0 \leq R_t^i &\leq Q_{t-1}^i, \quad i \in [1, M] \\ \sum_{i=1}^M R_t^i &\leq R^{max}(k_t), \end{aligned} \quad (3.13)$$

where Q_{t-1}^i is the number of packets in Q^i at the end of time frame $t-1$ with the definition of $Q_{t-1}^i \in Q_i := [0, B_i]$ and $R^{max}(k_t)$ denotes the maximum allowable number of packets transmitted per time frame at physical layer given channel state S_k at time frame t . Assuming that n_p packets can be accommodated during each time frame where n_p depends on the designer's choice, we have $R^{max}(k_t) = n_p \times R(k_t)$ where $R(k_t)$ is the symbol rate corresponding to channel state S_k . Therefore, we can get the recursions of the queue state for Q^i as

$$Q_t^i = \min(B_i, \max(0, Q_{t-1}^i - R_t^i) + A_t^i), \quad i = 1, 2, \dots, M \quad (3.14)$$

where A_t^i is the packets arrived at time frame t for Q^i , denoting the network traffic condition and obviously, it is independent with other system parameters. Therefore, we can isolate A_t^i when considering the system state transition and construct the finite state Markov chain system model with state pair $(K_t, Q_{t-1}^1, Q_{t-1}^2, \dots, Q_{t-1}^i, \dots, Q_{t-1}^M)$ to analyze the system behavior by combining (3.12) to (3.14).

3.3.2 Priority-Based Rate Allocation

As discussed earlier, the queue state recursion relies on the queue status at both current and previous time frame as well as the physical layer transmission data rate corresponding to current channel state. Therefore, the problem comes out to be how to allocate the data rate at physical layer to the multiple MAC layer queues according to their diverse QoS requirements.

To resolve this problem, we propose a priority-based rate allocation (PRA) algorithm, where multiple queues are assumed to have different priorities and the physical layer data rate is distributed to the multiple MAC layer queues proportionally with higher priority queue getting higher data rate. Mathematically, the relations between the data rates of different queues are defined as:

$$\begin{aligned} R_t^M &= \beta R_t^{k-1} = \beta^2 R_t^{k-2} = \dots = \beta^{M-1} R_t^1 \\ \sum_{i=1}^M R_t^i &\leq R^{max}(k_t) \end{aligned} \quad (3.15)$$

where β is called as *proportional weight*, adjusting which the data rate allocation process could be controlled. Combining (3.13) with (3.15), we get the constraints for the data rates of the multiple queues as

$$\begin{aligned} \frac{R_t^1(1 - \beta^M)}{1 - \beta} &\leq R^{max}(k_t) \\ R_t^M &= \beta R_t^{k-1} = \beta^2 R_t^{k-2} = \dots = \beta^{M-1} R_t^1 \\ 0 &\leq R_t^i \leq Q_{t-1}^i, \quad i \in [1, M]. \end{aligned} \quad (3.16)$$

To explain the PRA algorithm in detail, let A denote the set of the queues which are waiting for data rate allocation, where initially we set $A = \{Q^1, Q^2, \dots, Q^M\}$. To maximally utilize the physical layer resources while satisfying the constraints in (3.16), an iterative-based PRA implementation is shown as

Step a: Initialization: Set $A = \{Q^1, Q^2, \dots, Q^M\}$ and $R^{max}(k_t)$ according to current AMC mode.

Step b: For $Q^i \in A$, calculate $(R_t^i)'$ according to the following equation:

$$\begin{aligned} \sum_{Q^i \in A} (R_t^i)' &= R^{max}(k_t) \\ (R_t^i)' &= q^{M-i}(R_t^1)' \end{aligned} \quad (3.17)$$

Step c: If $\forall Q^i \in A$, $(R_t^i)' \leq Q_{t-1}^i$, set $R_t^i = (R_t^i)'$ and then, terminate the algorithm; otherwise, go to Step d.

Step d: Find $Q^i \in A$, where $(R_t^i)' \geq Q_{t-1}^i$, set $R_t^i = Q_{t-1}^i$, $A = A - \{Q^i\}$ and $R^{max}(k_t) = R^{max}(k_t) - R_t^i$;

Step e: If $A == \phi$, terminate the algorithm; Otherwise, go to Step b.

3.3.3 System Modeling Using Finite State Markov Chain

3.3.3.1 Derivation of state transition matrix

Given the state pair $(K_t, Q_{t-1}^1, \dots, Q_{t-1}^i, \dots, Q_{t-1}^M)$ derived above, we now formulate the state transition probability matrix P_t with its elements $P_{((k, q_1, \dots, q_M), (k', q'_1, \dots, q'_M))}$ which denotes the state transition probability from system state $(K_t, Q_{t-1}^1, \dots, Q_{t-1}^M)$ to system state $(K_{t+1}, Q_t^1, \dots, Q_t^M)$. Mathematically, the state transition probability can be computed by

$$P_{((k, q_1, \dots, q_M), (k', q'_1, \dots, q'_M))} = P_{k, k'} \cdot [P_{((q_1, \dots, q_M), (q'_1, \dots, q'_M)) | K=k'}], \quad (3.18)$$

where $P_{k, k'}$ is the channel state transition probability in P_c and $P_{((q_1, \dots, q_M), (q'_1, \dots, q'_M)) | K=k'}$ can be calculated as

$$P_{((q_1, \dots, q_M), (q'_1, \dots, q'_M)) | K=k'} = \prod_{i=1}^M P(Q_t^i = q'_i | Q_{t-1}^i = q_i, R_t^i = r_i), \quad (3.19)$$

where r_i represents the data rate allocated to queue Q^i . Using (3.12) and (3.14), we compute $P(Q_t^i = q'_i | Q_{t-1}^i = q_i, R_t^i = r_i)$ for Q^i as

$$P(Q_t^i = q'_i | Q_{t-1}^i = q_i, R_t^i = c_i) = \begin{cases} P(A_t^i = q'_i - \max\{0, q_i - r_i\}), & \text{if } 0 \leq q'_i < B_i \\ 1 - \sum_{0 \leq q'_i < B_i} P(Q_t^i = q'_i | Q_{t-1}^i = q_1, R_t^i = r_i), & \text{if } q'_i = B_i. \end{cases} \quad (3.20)$$

3.3.3.2 Stationary distribution of Markov chain

From the state transition matrix P_t , we calculate the stationary distribution of the Markov chain with definition:

$$\begin{aligned} \Pi(k, q_1, \dots, q_M) &= P(K = k, Q^1 = q_1, \dots, Q^M = q_M) \\ &:= \lim_{t \rightarrow \infty} P(K_t = k, Q_{t-1}^1 = q_1, \dots, Q_{t-1}^M = q_M). \end{aligned} \quad (3.21)$$

We define the stationary distribution row vector as

$$\mathbf{\Pi} = [\Pi(0, \dots, 0), \dots, \Pi(k, q_1, \dots, q_M), \dots, \Pi(K, B_1, \dots, B_M)]. \quad (3.22)$$

The stationary distribution of state pair $(K_t, Q_{t-1}^1, \dots, Q_{t-1}^i, \dots, Q_{t-1}^M)$ can be finally obtained by solving the following equations

$$\mathbf{\Pi} = \mathbf{\Pi} P_{sys}, \text{ and } \sum \mathbf{\Pi}(k, q_1, \dots, q_M) = \mathbf{1}. \quad (3.23)$$

3.4 System QoS Performance

Based on the stationary distribution obtained from (3.23), the QoS performance of the proposed system is analyzed, in terms of packet loss rate and average system delay. In

this section, we just take one of the multiple queues Q^i as an example and the rest can be processed in a similar way.

3.4.1 Packet Loss Rate

Since we assume a finite length queue at MAC layer, the new arriving packets will be dropped once the queue is full. Let P_d^i denote the dropping probability of Q^i . On the other hand, thanks to the searching-based channel partitioning, the packet error rate at physical layer constantly remains P_e . Because the packet loss of the system may be either caused by the packet dropping at MAC layer or by the transmission error at physical layer, the overall packet loss rate ζ^i of data in Q^i can be given by

$$\zeta^i = 1 - (1 - P_e)(1 - P_d^i). \quad (3.24)$$

Let D_t^i denote the number of packets dropped at time frame t for Q^i , where obviously D_t^i is determined by the number of packets at last time frame, the arrival packets and the transmitted packets at current time frame. Therefore, it can be given as

$$D_t^i = \max\{0, \max\{0, Q_{t-1}^i - R_t^i\} + A_t^i - B_t^i\}. \quad (3.25)$$

In the proposed model, we pursue the stable performance of the transmission system. Therefore, to get the stationary status of D_t^i , as $t \rightarrow +\infty$, we have

$$\begin{aligned} D^i &= \lim_{t \rightarrow +\infty} D_t^i \\ &= \lim_{t \rightarrow +\infty} \max\{0, \max\{0, Q_{t-1}^i - R_t^i\} + A_t^i - B_t^i\} \\ &= \max\{0, \max\{0, Q^i - R^i + A^i - B^i\}, \end{aligned} \quad (3.26)$$

where $A = \lim_{t \rightarrow +\infty} A_t^i$ and $Q = \lim_{t \rightarrow +\infty} Q_t^i$. According to the definition of dropping probability, we can obtain P_d^i as

$$\begin{aligned}
 P_d^i &= \lim_{T \rightarrow +\infty} \frac{\sum_{t=1}^T D_t^i}{\sum_{t=1}^T A_t^i} = \frac{E\{D^i\}}{E\{A^i\}} \\
 &= \frac{\sum_{a \in A^i, q^i=q} \max\{0, \max\{q - R^i\} + a - B^i\} \cdot P(A^i = a) \cdot [\Pi(k, q_1, \dots, q_M)]_{q_i \in B^i}}{\lambda T_f},
 \end{aligned} \tag{3.27}$$

where $P(A^i = a)$ is given by (3.12) and $\Pi(k, q_1, \dots, q_M)$ is the stationary distribution obtained through (3.23).

3.4.2 Average System Delay

Little's theorem [40] is used to describe the system delay, which is

$$\xi^i = \frac{\bar{Q}^i}{\lambda_{eq}^i T_f}, \tag{3.28}$$

where \bar{Q}^i is the average queue size of Q^i , and λ_{eq}^i denotes the average enqueued arrival rate, exclusive of the dropped packets. Evidently, $\lambda_{eq}^i = \lambda^i(1 - P_d^i)$ where P_d^i is the dropping probability in (3.27) and \bar{Q}^i can be obtained using the marginal distribution as

$$\bar{Q}^i = \sum_{q^i \in B_i} q \cdot \sum [\Pi(k, q_1, \dots, q_M)]_{q_i=q}. \tag{3.29}$$

3.5 Simulations

3.5.1 Parameter Setting

In this section, simulation results are provided to verify the proposed algorithm by measuring the stationary distribution. The un-coded M_n -QAM modulation transmission modes in Table 3.1 are used as the AMC modes at physical layer. As described in chapter 3.3.2, searching-based channel partitioning scheme is adopted where we set $P_e = 10^{-4}$. The channel is partitioned into six states ($N = 5$) corresponding to the transmission modes in Table 3.1, where state 1 refers to mode 0 which represents NULL mode while the other five states match the five transmission modes. In NULL mode, no packet is transmitted and it is mainly used to avoid the channel deep fading. Some other system parameters are set as follows:

- time frame length $T_f = 2\text{ms}$;
- system average received SNR $\gamma_0 = 20\text{dB}$;
- $n_p = 4$;
- Doppler frequency $f_d = 10\text{Hz}$.

Moreover, for convenience, we assume that there are three queues deployed at MAC layer, that is $M = 3$. The Poisson arrival rates of the three queues are considered to be the same where we set $\lambda^1 = \lambda^2 = \lambda^3 = 10^3$ (packets/sec). Moreover, same queue length is considered for all the three queues, i.e. $B_1 = B_2 = B_3$.

3.5.2 Simulation Results

We start with simulating the system QoS performance with different pre-defined packet error rate P_e . As shown in Fig. 3.6, as the increase of P_e , the packet loss rate firstly decreases

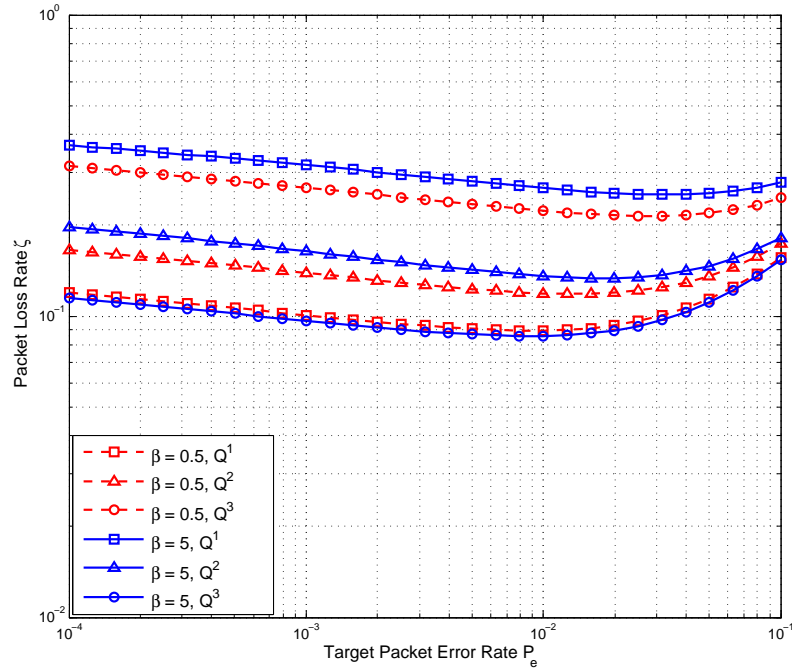


Figure 3.6: Packet loss rate under different pre-defined packet error rates.

and then increases after reaching the bottom. This indicates that when we design the system, an optimal P_e can be derived for a minimal packet loss rate. As for the packet loss rate of different queues, we can see that different queues have different packet loss rates according to their different priorities, due to the proposed PRA algorithm. Moreover, adjusting the proportional weight β , the priorities of the three queues change, and correspondingly the packet loss rate of the three queues changes as well.

Fig. 3.7 presents the average system delay of different queues regarding to different P_e , where we can see that with the increase of P_e , the average system delay of all the queues decreases. This is simply because the increase of physical layer packet error rate leads to more packets be transmitted and thus, the average system delay decreases as well. Furthermore, similar as what has been demonstrated in Fig. 3.6, different queues are provided with different average system delay, which can be further adjusted by configuring the proportional weight β .

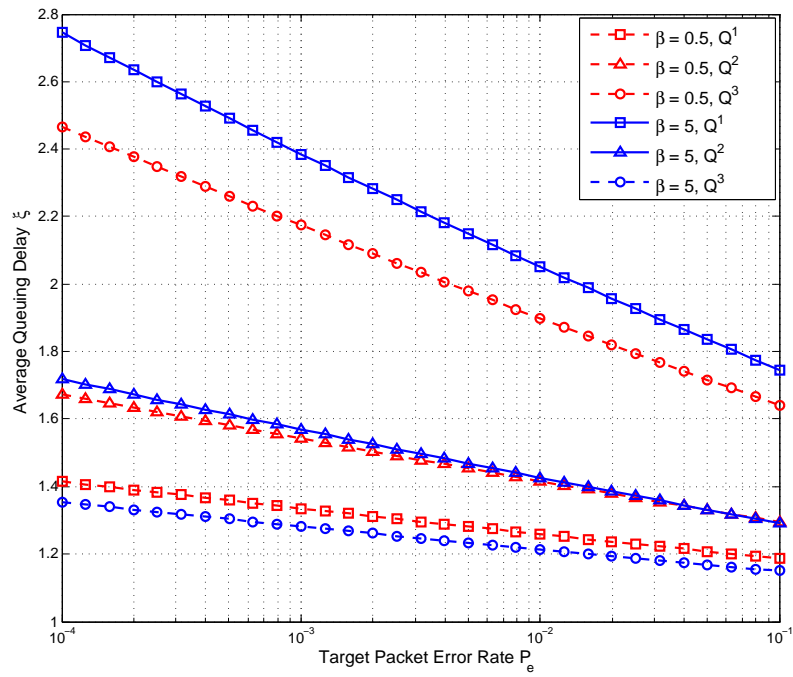


Figure 3.7: Average system delay under different pre-defined packet error rates.

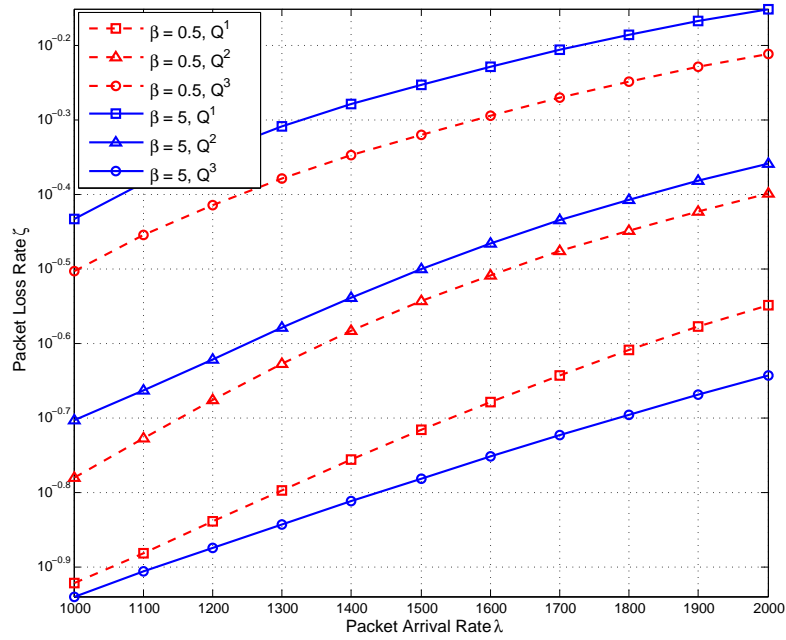


Figure 3.8: Packet loss rate under different traffic loads.

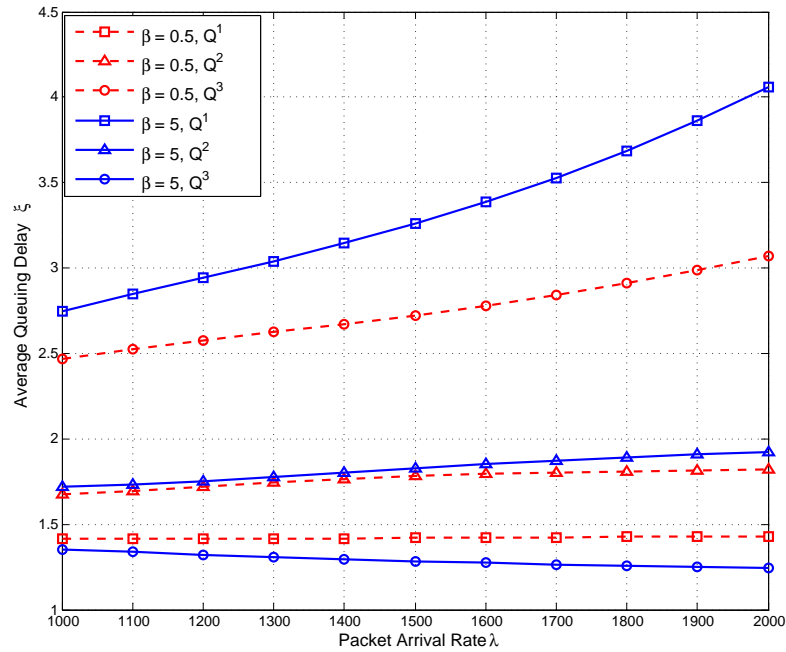


Figure 3.9: Average system delay under different traffic loads.

Then we get the system QoS performance under different traffic loads, that is when Poisson arrive rate λ^i varies. Fig. 3.8 shows the variation of the packet loss rate with different packet arrival rates. As we can see from Fig. 3.8, increasing the packet arrival rate leads to the increase of packet loss rate as well. More precisely, for $\beta = 5$, meaning that Q^1 has the highest priority, Q^3 has the lowest priority and the priority of Q^2 is in between, data in Q^1 gets the best packet loss rate performance, followed by the packet loss rate performance of Q^2 , while Q^3 has the worst performance. Furthermore, if we reverse the priorities of the three queues and set $\beta = 0.5$, the packet loss rate of the three queues reverses as well.

Finally, we analyze the average system delay with different packet arrival rates, as shown in Fig. 3.9. Apparently, with the slight increase of the packet arrival rate, the physical layer can transmit the packets from MAC layer in a timely manner and thus, the average system delay remains nearly unchanged. However, if we further increase the packet

arrival rate, when beyond the physical layer transmission capability, packets have to wait longer in the queue before they can be processed. Therefore, the average system delay increases. Moreover, physical layer authorizes more transmission of the queue with higher priority (such as Q^1 when $\beta = 5$ and Q^3 when $\beta = 0.5$ in our simulation case), reducing the average system delay of higher priority queue, and on the other hand, unavoidably resulting in the dramatic increase of the average system delay of lower priority queue.

3.6 Summary

To provide diverse QoS in wireless communications, a cross-layer finite state Markov chain system model has been proposed in this chapter, combining the multiple queues deployed at MAC layer with the physical layer FSMC channel. At physical layer, the time-varying channel was modeled by FSMC channel and then combined with the MAC layer queue status to construct the finite state Markov chain to model the communication system. To assure different queues with different QoS, a priority-based rate allocation was proposed to allocation the physical layer data rate to the multiple MAC layer queues, where different queues were assigned with different priorities and higher priority queue could obtain larger data rate for transmission, leading to the diverse QoS provision. Simulation results have demonstrated that the proposed system model were able to ensure different queues with different QoS, in terms of packet loss rate and average system delay.

Chapter 4

QoS Constrained Subcarrier Allocation in MU-OFDM system

Multuser-orthogonal frequency division multiplexing (MU-OFDM) system is being widely applied to provide diverse Quality of Service (QoS) for multiple users. In this chapter, in order to meet users' diverse QoS requirements in MU-OFDM system, a cross-layer dynamic subcarrier allocation algorithm is proposed, where users' MAC layer diverse QoS requirements and the subcarrier allocation at PHY layer are jointly considered. The MAC layer queue status is modeled as a finite-state Markov chain, using which the QoS constraints are translated to the minimal physical (PHY) layer data rate requirement of each user. A sub-optimal dynamic subcarrier allocation algorithm is then proposed not only to satisfy the physical layer data rate but also to significantly reduce the computational burden, aiming at maximizing system capacity.

4.1 Introduction

The demand of simultaneously supporting a large number of users with different QoS requirements in wireless communications is tremendously increasing. MU-OFDM system which allows multiple users transmit over different subcarriers per OFDM symbol at the same time, has been regarded as a potential candidate to meet this requirement [41].

Subcarrier allocation is one of the key challenges in MU-OFDM system and so far, two main categories of subcarrier allocation schemes have been proposed in literatures [42], namely static subcarrier allocation and dynamic subcarrier allocation. It has been widely recognized that dynamic subcarrier allocation overcomes its static counterpart in MU-OFDM system due to the variation of the channel gains of different subcarriers caused by the time-varying nature of wireless channels [43, 44]. By dynamically allocating subcarriers to different users according to their instantaneous channel state information (CSI), MU-OFDM system fully explores the channel diversity among users and thus, achieves an optimal system performance, constrained by the limited resources.

In both [45] and [46], authors proved that the system sum capacity could be maximized by assigning each subcarrier to the user with the best channel gain with the transmit power distributed by water-filling algorithm. However, fairness among users is not considered in these algorithms. Therefore, additional data rate constraints for each user were imposed to the optimization objective to achieve a fair performance [47, 48]. Nevertheless, all the above works only paid their attentions to physical layer and have rarely considered the MAC layer queue behavior as well as users' diverse QoS demands.

Motivated by guaranteeing diverse QoS for different users, we propose a two-step cross-layer dynamic subcarrier allocation algorithm in MU-OFDM system where every user desires different QoS. First, the MAC layer queue status is modeled as a finite-state Markov chain, whose stationary distribution is obtained to analyze the system QoS performance, using which MAC layer diverse QoS constraints can be translated to the minimal physical layer data rate of each user. Then, a dynamic subcarrier allocation algorithm is proposed to maximize the system capacity with the data rate constraints derived by MAC layer queue status model.

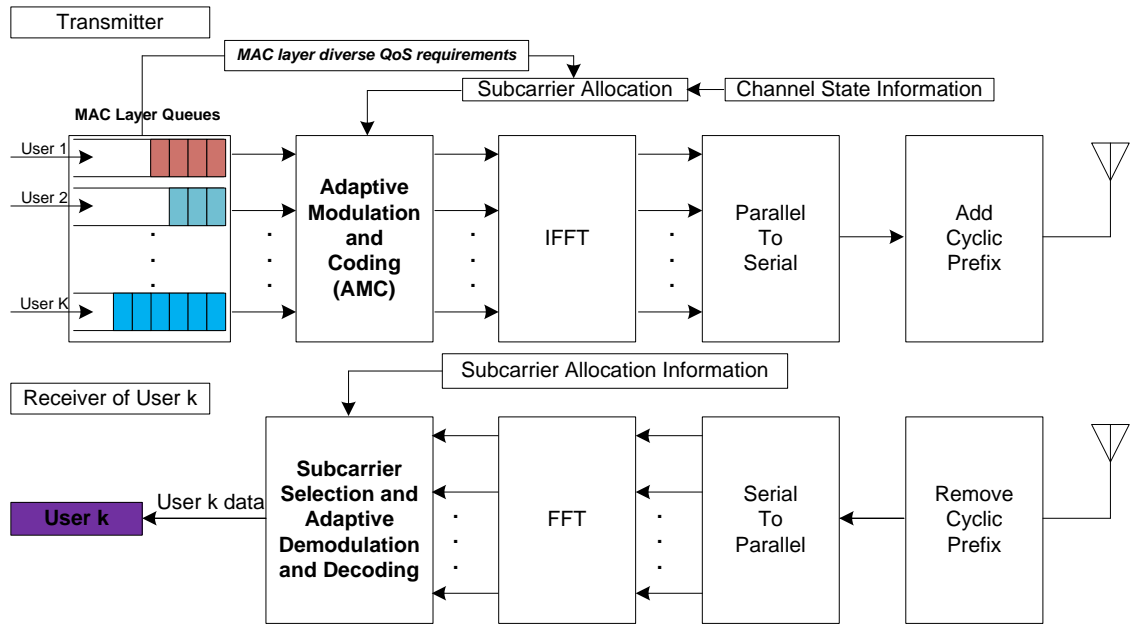


Figure 4.1: Multiuser OFDM system.

4.2 System Model

Similar as the system shown in Fig. 3.1, we consider the downlink transmission of a wireless network where base station (BS) is connected with multiple subscribers (SS). Every subscriber transmits different kinds of data and thus, requires different QoS. The base station is regarded as a multiuser OFDM system where each user corresponds to a subscriber in the network and OFDM modulation scheme is adopted at physical layer.

Fig. 4.1 shows a typical multiuser OFDM system where the transmitter is employed with K queues with queue k handling the data for user k . Perfect instantaneous channel state information obtained through the channel estimation at receiver is assumed to be available for both the transmitter and receiver. Based on MAC layer diverse QoS requirements as well as physical layer instantaneous CSI, the proposed subcarrier allocation algorithm assigns different users with the available subcarriers to form an OFDM symbol. The allocation information is then sent to all the users using a separate channel for the data

recovery at the receiver. Since we pursue a dynamic subcarrier allocation scheme, the allocation operation is triggered once either the QoS requirements or the instantaneous CSI change.

Moreover, we assume that the system operates on a frame by frame basis with each frame a fixed time duration T_f . For the data of user k , packets arriving during time frame t ($[tT_f, (t + 1)T_f)$) are enqueued by MAC layer queue k at time slot $(t + 1)T_f$ and will be served in next time frame. Adaptive modulation and coding (AMC) updated according to instantaneous CSI is used at transmitter to provide the system a stable physical layer performance, i.e. a fixed packet error rate at physical layer for each subcarrier $\text{PER} \equiv P_0$.

4.3 Problem Formulation

We assume the MU-OFDM system containing a total of K users with N subcarriers and the transmit power is assumed to be limited with maximum value P_t . The objective of the proposed algorithm is to maximize the system capacity with the constraints of available transmit power P_t as well as MAC layer diverse QoS requirements, in terms of packet loss rate and average queue size.

Mathematically, the optimization problem can be formulated as

$$\begin{aligned} & \max \sum_{k=1}^K \sum_{n=1}^N \frac{\rho_{k,n}}{N} \log_2 \left(1 + \frac{p_{k,n} h_{k,n}^2}{N_0 \frac{BW}{N}} \right) \\ & \text{subject to :} \\ & \text{C1: } \sum_{k=1}^K \sum_{n=1}^N p_{k,n} \leq P_t \\ & \text{C2: } p_{k,n} \geq 0, \forall k, \forall n \\ & \text{C3: } \rho_{k,n} \in \{0, 1\}, \forall k, \forall n \\ & \text{C4: } \sum_{k=1}^K \rho_{k,n} = 1, \forall n \\ & \text{C5: } \zeta^k \leq P_{max}^k, \forall k \\ & \text{C6: } Q_{avg}^k \leq Q_{max}^k, \forall k \end{aligned} \tag{4.1}$$

where N_0 is the power spectral density (PSD) of additive white Gaussian noise (AWGN) and BW is the available transmission bandwidth. $p_{k,n}$ denotes the transmit power allocated to user k in subcarrier n and $h_{k,n}$ is the channel gain for user k using subcarrier n . As for $\rho_{k,n}$, it can only be either 1 or 0, indicating whether subcarrier n is occupied by user k . Moreover, C1 is the total transmit power constraint while C4 shows that each subcarrier can only be used by one user. C5 and C6 are the MAC layer diverse QoS constraints where P_{max}^k and Q_{max}^k are the allowable maximum packet loss rate and average queue size of user k respectively.

4.4 Proposed Cross-Layer Dynamic Subcarrier

Allocation

In this section, the proposed cross-layer dynamic subcarrier allocation algorithm which jointly considers MAC layer diverse QoS constraints and physical layer subcarrier allocation scheme, is explained in detail. We first introduce the finite-state Markov chain queue status model at MAC layer which enables us to derive the minimal physical layer data rate for each user from the diverse QoS constraints. Then, with the physical layer data rate constraints, a sub-optimal dynamic subcarrier allocation algorithm is proposed to maximize the system capacity while making the computing time still under control.

4.4.1 MAC Layer Queue Status Model

Since all the users in MU-OFDM system have similar situation, we just choose one user as an example and the rest can be analyzed in the same way. Assume that for a certain user, it has a finite length (B) queue Q which works in first-in-first-out (FIFO) operation mode.

4.4.1.1 Queuing model using finite state Markov Chain

Let A_t denote the number of packets arriving at time frame t for Q , where we assume that A_t is Poisson distributed with parameter λT_f , satisfying (3.12).

Let R (packets/time frame) denote the physical layer data rate, thus we can get the recursion of the queue state as

$$Q_t = \min(B, \max(0, Q_{t-1} - R) + A_t) \quad (4.2)$$

where Q_t and Q_{t-1} denote the number of packets in Q at the end of time frame t and $t - 1$ respectively.

Let $\{S_i\}, i = 1, 2, \dots$ denote a Markov process and we define the queue in state S_b when its size equals b , where $b \in [0, B]$ and $S_b \in S = \{S_0, S_1, \dots, S_B\}$. Combining (3.12) with (4.2), we get the state transition probability p_{sl} which represents the transition probability from state S_s to S_l as follows:

$$p_{sl} = Pr\{S_{i+1} = l | S_i = s\} = \begin{cases} P(A_t = l - \max(0, s + R)), & \text{if } l < B \\ 1 - \sum_{0 \leq n < B} Pr\{S_{i+1} = n | S_i = s\}, & \text{if } l = B \end{cases} \quad (4.3)$$

Thus, the $(B + 1) \times (B + 1)$ state transition matrix \mathbf{P}_t is obtained as

$$\mathbf{P}_t = \begin{bmatrix} p_{00} & p_{01} & \dots & p_{0B} \\ p_{10} & p_{11} & \dots & p_{1B} \\ \vdots & \vdots & \ddots & \vdots \\ p_{B0} & p_{B1} & \dots & p_{BB} \end{bmatrix} \quad (4.4)$$

where all the elements are calculated by (4.3).

Let $\pi = [\pi_0, \pi_1, \dots, \pi_B]$ denote the stationary distribution of S_i and it can be obtained by solving the following balance equation

$$\pi \mathbf{P}_t = \pi \quad (4.5)$$

where π satisfies the uniform constraint, that is $\sum_{b=0}^B \pi_b = 1$.

4.4.1.2 QoS performance analysis

Based on the stationary distribution π obtained in (4.5), the detailed procedure of analyzing MAC layer QoS performance in terms of packet loss rate and average queue size is given in a similar way as (3.24) to (3.29),

- Packet loss rate ζ :

$$\begin{aligned} \zeta &= 1 - (1 - P_d)(1 - P_0) \\ &= \frac{\lambda T_f - \sum_{a \in A, b \in [0, B]} \max\{0, \max\{b - R\} + a - B\} \cdot P(A = a) \cdot \pi(b)}{\lambda T_f} (1 - P_0) \end{aligned} \quad (4.6)$$

where $A = \lim_{t \rightarrow +\infty} A_t$, $Q = \lim_{t \rightarrow +\infty} Q_t$, $P(A = a)$ is given by (3.12) and $\pi(q)$ is the stationary distribution in (4.5).

- Average queue size Q_{avg} :

$$Q_{avg} = \sum_{b \in [0, B]} b \cdot \pi(b) \quad (4.7)$$

So far, we have modeled MAC layer queue status as a finite-state Markov chain where MAC layer QoS performance is determined by the physical layer data rate. Therefore, we can translate MAC layer diverse QoS constraints to physical layer minimal data rate requirement of each user to constrain the subcarrier allocation at physical layer, instead of directly using MAC layer diverse QoS requirements to do so.

4.4.2 Dynamic Subcarrier Allocation at Physical Layer

In order to achieve an optimal solution for (4.1), ideally subcarriers and transmit power allocation should be jointly considered which however, leads to long computing time. Moreover, as we aim at a dynamic subcarrier allocation, subcarrier allocation scheme should be updated once the channel condition or MAC layer QoS requirements change. This further aggravates the computational burden. Consequently, joint optimal solution may be not feasible in practical system and sub-optimal lower-complexity algorithm is considered as a more suitable candidate.

For the sake of reducing the computing time, the subcarrier and transmit power allocation are separately considered and we only focus on the subcarrier allocation part. As for the transmit power allocation, we adopt the optimal power distribution for a fixed subcarrier allocation algorithm proposed in [50].

Besides, to provide the diverse QoS to different users, in the proposed algorithm, the MAC layer QoS requirements are involved in the physical layer subcarrier allocation. More specifically, for user k , its MAC layer packet loss rate constraint P_{max}^k as well as average queue size constraint Q_{max}^k are translated to the minimal data rate requirement R_{min}^k at physical layer, using the MAC layer queue status model discussed earlier. Then, we conduct the proposed subcarrier allocation algorithm constrained by the data rate requirement for each user instead of the diverse QoS constraints, i.e. $R_k \geq R_{min}^k, k = [1, 2, \dots, K]$ where R_k is the physical layer data rate of user k .

We first assume equal transmit power distribution when conducting the proposed subcarrier allocation algorithm and define $H_{k,n} = h_{k,n}^2/N_0(\text{BW}/N)$ as the channel-to-noise ratio of user k in subcarrier n . Let Ω_k denote the set of subcarriers allocated to user k and U denote the users waiting for subcarrier allocation. The data rate of user k denoted as R_k is given by

$$\begin{aligned} R_k &= \sum_{n=1}^N \frac{p_{k,n}}{N} \log_2 \left(1 + \frac{p_{k,n} h_{k,n}^2}{N_0 \frac{\text{BW}}{N}} \right) \\ &= \sum_{n \in \Omega_k} \frac{\log_2 \left(1 + \frac{p_{k,n} h_{k,n}^2}{N_0 \frac{\text{BW}}{N}} \right)}{N} \end{aligned} \quad (4.8)$$

Based on the above assumptions, the details of the proposed cross-layer dynamic subcarrier allocation algorithm are given as follows

1. Initialization and minimum physical layer data rate derivation

set $U = \phi$ and $A = \{1, 2, \dots, N\}$

for $k = 1$ to K

(a) get MAC layer QoS constraints, P_{max}^k and Q_{max}^k ;

(b) using the MAC layer queue status model, find out the minimal physical layer data rate R_{min}^k , with the constraints in a);

(c) set $R_k = 0$, $\Omega_k = \phi$ and $U = U \cup \{k\}$.

2. For $k = 1$ to K

(a) find n satisfying $|H_{k,n}| \geq |H_{k,j}|, \forall j \in A$;

(b) update Ω_k, A where $\Omega_k = \Omega_k \cup n$ and $A = A - \{n\}$;

(c) update R_k according to (4.8);

(d) if $R_k \geq R_{min}^k$, $U = U - \{k\}$.

3. While $A \neq \phi$ and $U \neq \phi$

(a) find k satisfying $R_k/R_{min}^k \leq R_i/R_{min}^i, \forall i \in U$;

(b) update Ω_k, A where $\Omega_k = \Omega_k \cup n$ and $A = A - \{n\}$;

(c) update R_k according to (4.8);

(d) if $R_k \geq R_{min}^k$, $U = U - \{k\}$.

The basic principle of the proposed algorithm is to use the subcarriers with high $H_{k,n}$ as much as possible for each user and assign users different priorities according to their QoS requirements. To get better performance, optimal transmit power allocation algorithm for a fixed subcarrier allocation proposed in [50] is adopted as the power allocation scheme after we get the subcarrier allocation result.

4.5 Simulations

4.5.1 Parameter Setting

In this section, simulation results are provided to validate the proposed algorithm. The wireless channel is considered as a frequency-selective with six independent Rayleigh multipaths where each multipath is modeled as Clarke's flat fading [51]. The power delay profile is considered to be exponentially decaying represented by e^{-2I} where I is the multipath index. Accordingly, the relative power of the six multipath components are $[0, -8.69, -17.37, -26.06, -34.74, -43.43]$. We also assume that there are total BW = 1Hz transmission bandwidth and $P_{max}^t = 1W$ transmit power available. The physical layer packet error rate is set as $P_0 \equiv 10^{-4}$ and the time frame length is $T_f = 2ms$.

Besides, the MU-OFDM system is assumed to contain $K = 4$ users sharing $N = 256$ subcarriers. For simplicity, the corresponding four MAC layer queues are considered to be equal length, i.e. $B_i = 50, i = [1, 2, 3, 4]$. However, different users are allowed to have different traffic loads which are represented by their different Poisson arrival rates, i.e.

$$[\lambda_1, \lambda_2, \lambda_3, \lambda_4] = [4 \times 10^3, 6 \times 10^3, 8 \times 10^3, 1 \times 10^4](\text{packets/sec}). \quad (4.9)$$

4.5.2 MAC Layer Queue Performance

First, packet loss rates with different physical layer data rates for different users are simulated. As shown in Fig. 4.2, it is clear that packet loss rate ζ decreases with the increasing of physical layer data rate R and user with heavier traffic load, i.e. a larger λ , suffers larger packet loss rate. One point needs to be emphasized is that if we keep increasing the physical layer data rate R , packet loss rate ζ will approach 10^{-4} which is the pre-defined packet

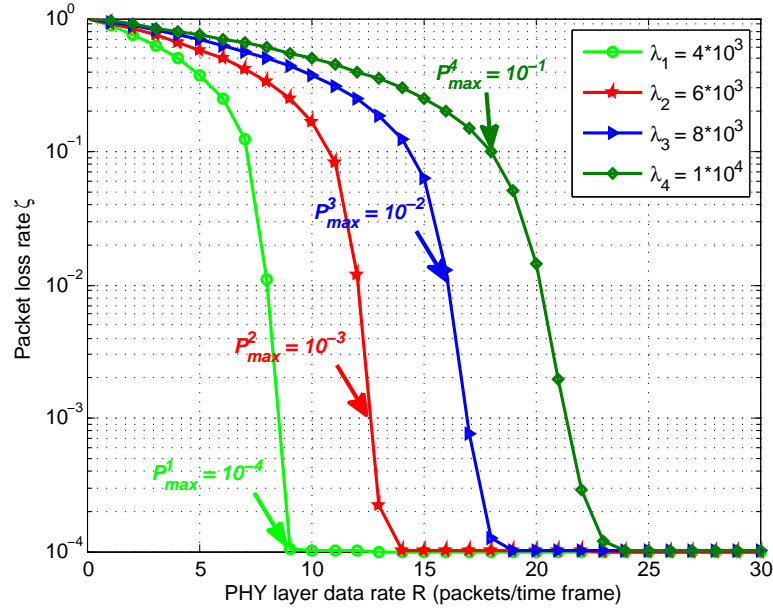


Figure 4.2: Packet loss rate under different physical layer data rates.

error rate P_0 . In this case, the whole system packet loss rate is dominated by the packet error rate at physical layer and the packet dropping at MAC layer is neglectable.

Fig. 4.3 shows the MAC layer average queue size under different data rates for different users, where we can see with the increasing of physical layer data rate, the queues get a shorter average queue size due to the transmission of more data within each time frame. Similarly with Fig. 4.2, with heavier traffic load, the user gets larger average queue size which implies all the data in the queue experience longer delay. Furthermore, if we further increase the physical layer data rate, the average queue size of each user tends to be the stable value which equals the number of packets arrived during each time frame λT_f . In this case, the packets in the queue only sustain one time frame delay and this situation is the optimal one, leading to the shortest delay.

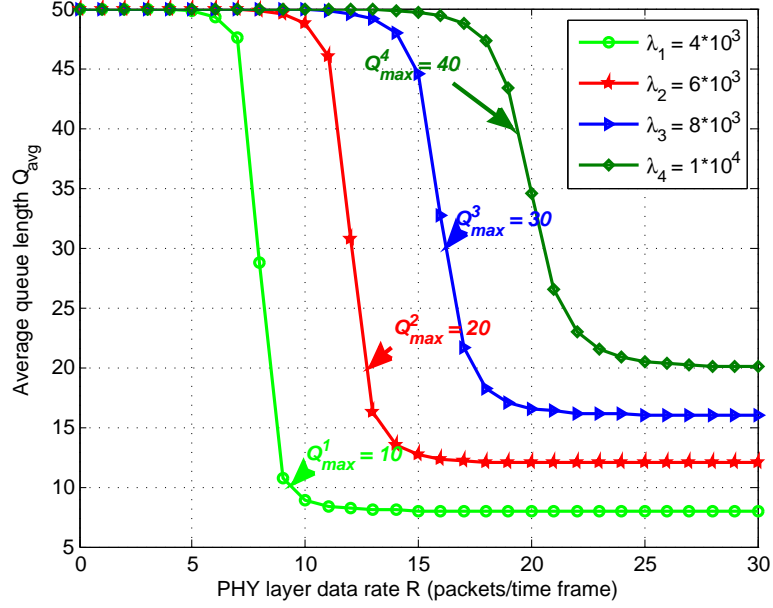


Figure 4.3: MAC layer average queue size under different physical layer data rates.

4.5.3 Physical Layer Subcarrier Allocation Performance

After we construct the MAC layer finite state Markov chain queue status model, we conduct the subcarrier allocation performance simulation following the steps in chapter 4.4.2. We set the packet loss rate constraint for each user as

$$[P_{max}^1, P_{max}^2, P_{max}^3, P_{max}^4] = [10^{-4}, 10^{-3}, 10^{-2}, 10^{-1}] \quad (4.10)$$

and the average queue size requirements of the four users are

$$[Q_{max}^1, Q_{max}^2, Q_{max}^3, Q_{max}^4] = [10, 20, 30, 40]. \quad (4.11)$$

For convenience, we assume that the data rate at physical layer can only be integers. Deriving from Fig. 4.2 and Fig. 4.3, we can easily get the minimal data rate requirements

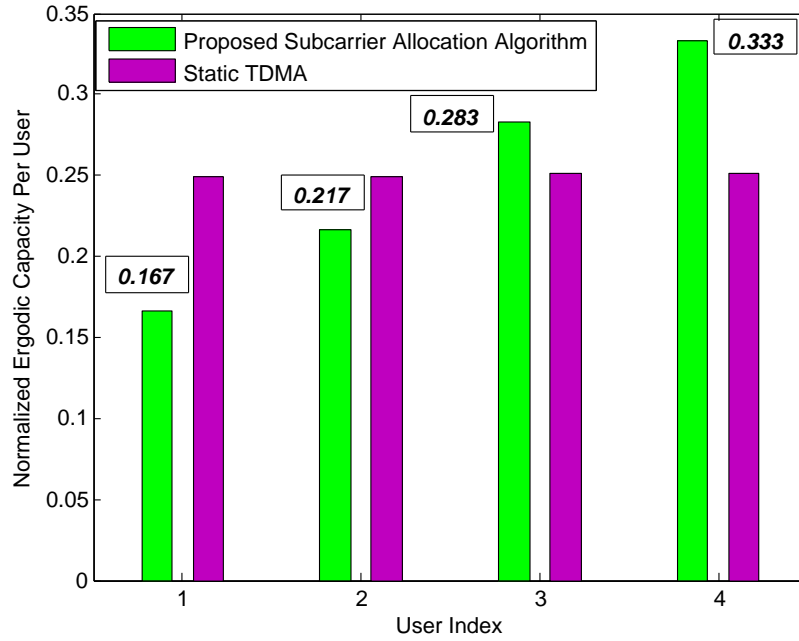


Figure 4.4: Normalized ergodic sum capacity distribution among users.

of the four users as

$$[R_{min}^1, R_{min}^2, R_{min}^3, R_{min}^4] = [9, 13, 17, 20](\text{packets/time frame}). \quad (4.12)$$

The subcarrier allocation simulation result is shown in Fig. 4.4 where we also simulate static TDMA subcarrier allocation mechanism for comparison. As depicted in Fig. 4.4, since the subcarriers in static TDMA are equally assigned to each user, the system capacity for each user is similar. However, using the proposed physical layer dynamic subcarrier allocation algorithm, the system capacity is distributed among all the users according to their different minimal physical layer data rate requirements and thus, MAC layer diverse QoS constraints are satisfied.

4.6 Summary

In this chapter, we have proposed a cross-layer dynamic subcarrier allocation algorithm in multiuser-OFDM system, where MAC layer diverse QoS requirements were introduced to constrain the subcarrier allocation at physical layer. The MAC layer queue status was modeled as a finite-state Markov chain and system QoS performance under different physical layer data rates was simulated. Based on the obtained queue status model, the MAC layer diverse QoS constraints were translated to the minimal physical layer data rate requirements. Then, knowing the perfect instantaneous CSI, we conducted the sub-optimal low-complexity subcarrier allocation according to users' different data rate requirements. Simulation results demonstrated that using the proposed MAC layer queue status model, we could get the minimal data rate requirement of each user from its QoS constraint and this requirement was met by using the proposed subcarrier allocation algorithm.

Chapter 5

QoS Oriented Channel Assignment in IEEE 802.11 WLANs

Channel assignment is of great importance for successfully designing and operating IEEE 802.11 wireless local area networks (WLANs). Aiming at providing the users a stable QoS performance and meanwhile, solving the problem of frequency scarcity in dense WLANs, a channel assignment algorithm is proposed in this chapter with the exploration of the partially overlapped channels for additional frequency resources. In the proposed algorithm, we first introduce a user number estimation scheme at physical layer where the number of users in IEEE 802.11 channels is obtained by determining the number of estimated channel impulse responses (CIRs). Then, based on the user number information, a dynamic channel assignment scheme is presented to maximize the system capacity with all the IEEE 802.11 channels considered and the interferences caused by the channel partial overlap is mathematically evaluated and involved. Moreover, users' QoS requirements are used to trigger the channel assignment for system QoS maintenance.

5.1 Introduction

IEEE 802.11-based wireless access technology, which is known as Wi-Fi, has been widely deployed in local area networks recently. This brings the convenience of promising services to the users, while on the other hand, also raises the issues like the coexistence of

more and more access points (APs). Therefore, a large number of APs have to share the limited IEEE 802.11 channels, leading to the severe interferences among neighboring APs and consequently, the degradation of system performance.

Allocating the limited IEEE 802.11 channels to the multiple APs, as one of the major problems in designing WLANs, has drawn increased research attentions [52, 53, 54], which can be generally divided into two categories, namely centralized schemes [53] and distributed schemes [54]. In centralized based algorithms, a network controller is deployed to collect the network information and allocate the available channels to all the APs for a global optimal performance, while in the distributed schemes, every AP acts individually and determines which channel to occupy, such that local optimal performance can be achieved. Nowadays, due to the lack of coordination and communications among APs in WLANs, it has been widely recognized that distributed schemes overcome their centralized counterparts.

In [55], Luo and Shankaranarayanan proposed a low-complexity distributed channel assignment scheme, named as LS scheme, to offer an improved overall throughput, where it assumes that the knowledge of the throughput function is known in advance to the APs, which makes it less practical in some situations. Regarding to this, the authors in [56] simplified the problem and proved that by choosing the channel with the minimum number of users, similar results can be also achieved as that in [55]. Moreover, an extended Kalman filter estimator was introduced in this paper to obtain the number of users, which is pivotal for most of the channel assignment algorithms.

The drawbacks of the major existing channel assignment schemes, however, can be summarized as follows:

- The number of users which is the key factor affecting the channel assignment algorithms, is obtained either through the beacon frame from APs or the MAC layer

information [56, 57, 58, 59], i.e. probability of collision. This not only aggregates the burden of upper layer structure design, but more importantly, causes long system latency. Therefore, those algorithms are not suitable to some high-dynamic environments.

- Only the three non-overlapped channels in IEEE 802.11 are examined, and this is becoming a sever problem due to the increasing density of WLANs.

Motivated by the above challenges, in this chapter, we first estimate the user number in IEEE 802.11 channels by determining the number of different CIRs. This method is implemented at physical layer without any affects to the upper layer structure and the time responsiveness can also be greatly improved, given that the CIRs are obtained promptly. To reduce the impact of CIR estimation noise, we introduce an adaptive noise elimination threshold, with which the impact of CIR estimation noise can be mitigated. Moreover, when distinguishing the terminals according to their CIR differences, an adaptive CIR determination threshold determined by both the number of significant paths and the SNR is also achieved, to further improve the accuracy of the proposed algorithm.

Then, we extend the work in [56] to solve the problem of frequency scarcity by not only utilizing the non-overlapped channels, but also exploiting the partially overlapped channels. In our proposed algorithm, a new optimization objective, called *Equivalent User Number* (EUN), is defined for each channel where the EUN combines the number of users in that channel and the interferences from the partially overlapped channels, and the AP is assigned with the channel which has the minimum EUN, rather than the channel with the minimum user number [56]. Consequently, not only the problem of frequency scarcity is solved, but also could the system throughput be greatly improved.

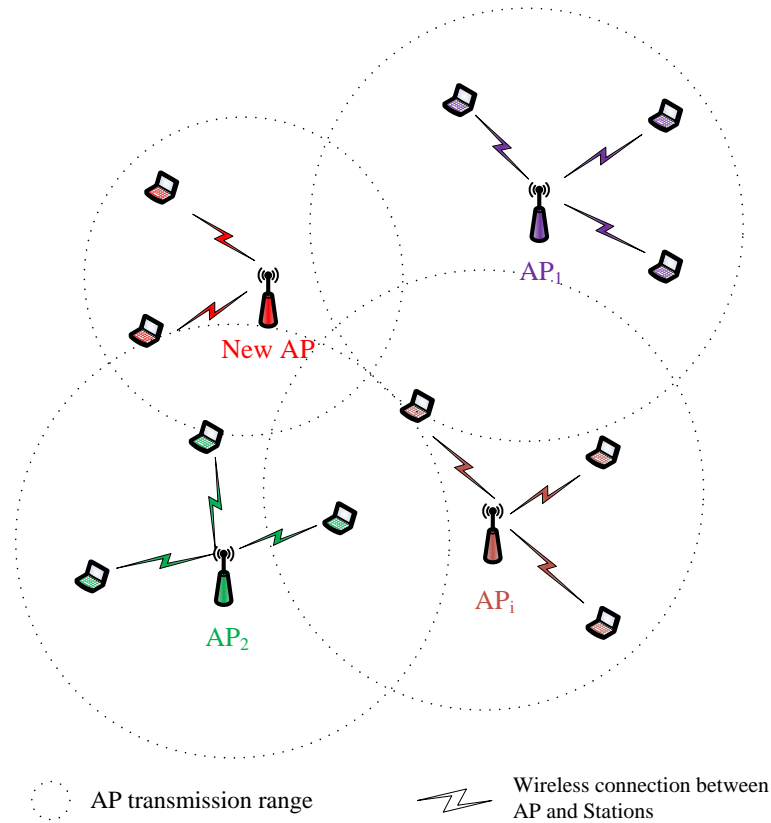


Figure 5.1: Typical infrastructure-based IEEE 802.11 WLAN with AP transmission range overlap.

5.2 System Model

The considered typical infrastructure-based IEEE 802.11 WLAN network system is shown in Fig. 5.1, where we assume that N_{AP} access points (APs) coexist in a common area, with multiple users attached. Each AP works on one of the IEEE 802.11 channels with the neighboring APs' their transmission ranges overlapped. Therefore, interferences exist between two APs working on the partially overlapped channels with the transmission range overlap. We also assume that users are assumed to be randomly deployed, and thus undergo different multipath fading, leading to their distinctive associated CIRs.

Moreover, as defined in IEEE 802.11a/g/n, prior to a group of OFDM data symbols in physical layer data frame, preambles are inserted for receiver synchronization and CIR

estimation. In addition, to eliminate the inter-symbol interference (ISI), each OFDM symbol is preceded by a cyclic prefix (CP), which contains the last N_{cp} samples of the symbol.

5.3 CIR-Based User Number Estimation

5.3.1 Physical Layer Model

In our proposed algorithm, we use the number of different CIRs observed in the shared channel to determine the number of users where we assume a constant user number during each estimation phase with the static position of the users. Considering the potential collision in IEEE 802.11 networks, the received signal may be the superposition of one or multiple simultaneously arriving signals from different users. For better estimation accuracy, we discard the superposed received signals with severe CIR estimation noise and only consider the collision-free period.

The time axis is slotted into CIR observation windows and the i -th window which represents time interval $[D_i, D_i + \zeta]$ where D_i is the start time of this window and ζ denotes the constant window duration equaling to the physical layer frame length [60], is defined as

$$\Pi(D_i) = u(t - D_i) - u(t - (D_i + \zeta)), \quad (5.1)$$

where $u(\cdot)$ denotes the unit step function, given as [61]

$$u(t - t_0) = \begin{cases} 1 & t \geq t_0 \\ 0 & t < t_0 \end{cases}. \quad (5.2)$$

The time window is then applied to the received signals and only the signals received during the collision-free observation windows are selected for further processing.

Therefore, with the time reference determined by the preambles in IEEE 802.11 [60], the received signal in a certain collision-free observation window can be expressed as

$$\begin{aligned} y_{D_i} &= \Pi(D_i) \cdot \sum_{m=1}^U \sum_{D_j \in T_m} x_{D_j}^m \otimes h_{D_j}^m + w_{D_i} \\ &= x_{D_i}^u \otimes h_{D_i}^u + w_{D_i}, \end{aligned} \quad (5.3)$$

where w_{D_i} represents zero-mean white complex Gaussian noise with variance σ_w^2 , T_m denotes the collection of the transmission active time of user m , and $h_{D_j}^m$ is the CIR of user m during the j -th observation window, which remains unchanged due to the assumption of slow fading channel model. However, the variation of h^m among different observation windows is allowed, i.e. $h_{D_j}^m$ and $h_{D_{j+1}}^m$ may be different. As for $x_{D_i}^u$, it denotes the single transmitted signal from user u in the i -th observation window, and $h_{D_i}^u$ is the associated CIR, which for brevity will be written as h in the rest of this letter and can be mathematically expressed as

$$h(t, \tau) = \sum_{l=0}^{L-1} a_l \delta(t - l\Delta_\tau), \quad (5.4)$$

where t is the observation time, L is the length of h , and $l\Delta_\tau$ and a_l are the delay and channel gain of the l^{th} multipath component respectively where a_l is modeled by a complex Gaussian random variable with zero mean and variance σ_l^2 , i.e. $a_l \sim N_c(0, \sigma_l^2)$.

5.3.2 LS Channel Estimation

In the considered OFDM system, Comb-type pilots are inserted into each OFDM and simple Least Squares (LS) channel estimation is adopted to obtain the frequency domain CIR

H [63], shown as

$$\begin{aligned} H &= [h_p(0)h_p(1)\dots h_p(N_p - 1)] \\ &= X_p^{-1}Y_p \\ &= \left[\frac{Y_p(0)}{X_p(0)} \frac{Y_p(1)}{X_p(1)} \dots \frac{Y_p(N_p - 1)}{X_p(N_p - 1)} \right], \end{aligned} \quad (5.5)$$

where N_p is the length of pilots while X_p and Y_p are the transmitted and received pilots respectively.

Then, inverse fast Fourier transform(IFFT) is then imposed to H to get the time domain CIR h . Moreover, we also consider two types of normalization related to CIR, i.e. time delay normalization and amplitude normalization, as shown in [62] and thereafter, h is used as the normalized ideal CIR.

5.3.3 Mitigation of CIR Estimation Noise

In the presence of additive white Gaussian noise (AWGN), the noise-imposed CIR \hat{h} is given by

$$\hat{h}_l = \begin{cases} h_l + n_e, & \text{if } l \in [0, L - 1] \\ 0, & \text{otherwise} \end{cases}, \quad (5.6)$$

where n_e represents the estimation noise which affects both the strong and weak paths. Therefore, mitigation of the noise impact is necessary to improve the accuracy of the obtained CIR.

In this chapter, as shown in Fig. 5.2, an adaptive noise elimination threshold is applied to mitigate the impact of the noise where the estimated CIR in (5.6) can be rewritten as

$$\hat{h}_l^{Th} = \begin{cases} \hat{h}_l, & \text{if } |\hat{h}_l| \geq \theta_{th} \\ 0, & \text{otherwise} \end{cases}, \quad (5.7)$$

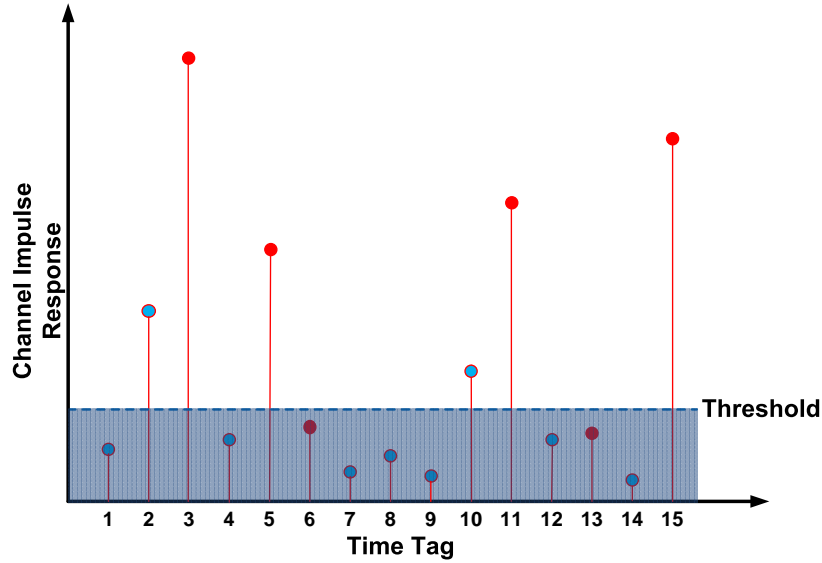


Figure 5.2: Threshold to eliminate the environment noise.

where the noise threshold θ_{th} is determined by minimizing the mean square error (MSE) of the estimation errors, show as

$$\theta_{th} = \arg \min_{\theta_{th}} MSE = \sum_{l=0}^{L-1} \mathbf{E} \left\{ |h_l - \hat{h}_l^T h|^2 \right\}. \quad (5.8)$$

A sub-optimal resolution for (5.8) has already been given in [64] in the absence of the knowledge of the channel statistic, that is

$$\theta_{th} \approx \sqrt{\sigma_N^2 \ln(N_p/P_{far})}, \quad (5.9)$$

where P_{far} is the false alarm rate, pre-defined by the users according to their system requirements and N_p is the length of preamble. As for the noise variance σ_N^2 , it can be given by exploiting the redundancy introduced by the CP in OFDM systems [65],

$$\sigma_N^2 = \frac{1}{2M(N_{cp} - L)} \sum_{v=0}^{M-1} \sum_{m=L}^{N_{cp}-1} Y(v, m), \quad (5.10)$$

where N is the number of subcarriers in each OFDM symbol, M is number of OFDM symbols in the training window and $Y(v, m)$ is given as

$$Y(v, m) = |y(v(N + N_{cp}) + m) - y(v(N + N_{cp}) + N + m)|^2. \quad (5.11)$$

5.3.4 Hypothesis Testing for CIR Differentiation

To judge whether \hat{h}_N^{Th} and \hat{h}_E^{Th} are from the same terminal or not, a binary hypothesis testing is formulated as

$$\begin{aligned} H_0 : \hat{h}_N^{Th} &= \hat{h}_E^{Th}; \\ H_1 : \hat{h}_N^{Th} &\neq \hat{h}_E^{Th}, \end{aligned} \quad (5.12)$$

where H_0 means that \hat{h}_N^{Th} and \hat{h}_E^{Th} are the same, indicating that they belong to the same terminal, while H_1 indicates they are associated with different terminals.

Due to the time varying environment, the ideal adjacent CIRs on the same path are different but correlated, modeled by an autoregressive model of order 1 (AR-1) [66],

$$h_l(i) = \eta h_l(i-1) + \sigma_l u_l \sqrt{1 - \eta^2}, \quad l \in [0, L-1], \quad (5.13)$$

where η is the AR coefficient, indicating the correlation of two consecutive CIRs on the same path, and u_l is a zero-mean complex Gaussian random variable with variance 1. Herein, we just take path l as an example and the rest can be analyzed in a similar way.

According to [66], the probability density function (PDF) of the test statistic under hypothesis H_0 and H_1 is given by

$$\begin{aligned} H_0 : T_l &\sim N_c(\underline{0}, \sigma_{H_0, l}^2 \mathbf{I}); \\ H_1 : T_l &\sim N_c(\mu \mathbf{I}, \sigma_{H_1, l}^2 \mathbf{I}), \end{aligned} \quad (5.14)$$

where T_l is a test statistic under hypothesis testing, exploiting the characteristics of the difference between \hat{h}_N^{Th} and \hat{h}_E^{Th} on the l^{th} path, while μ , $\sigma_{H_0,l}^2$ and $\sigma_{H_1,l}^2$ are calculated by

$$\begin{aligned}\mu &= \mathbf{E}[h_{E,l}] - \mathbf{E}[h_{N,l}] \\ \sigma_{H_0,l}^2 &= 2(1 - \zeta)\sigma_{N,l}^2 + 2\sigma_N^2 \\ \sigma_{H_1,l}^2 &= \sigma_{E,l}^2 + \sigma_{N,l}^2 + 2\sigma_N^2.\end{aligned}\tag{5.15}$$

where $\sigma_{E,l}^2$, $\sigma_{N,l}^2$ and σ_N^2 represent the variance of a complex Gaussian random variable.

5.3.5 Adaptive CIR Determination Threshold

Based on (5.7), the difference between the two noise-mitigated CIRs is given by

$$\Delta_{\text{CIR}} = \frac{1}{\gamma^2} \sum_{l=0}^{L-1} |\Delta \hat{h}_l^{Th}|^2 \tag{5.16}$$

$$= \frac{1}{\gamma^2} \sum_{l \in S_N \cup S_E} |\hat{h}_{N,l}^{Th} - \hat{h}_{E,l}^{Th}|^2, \tag{5.17}$$

where γ^2 is the variance for normalization. S_N and S_E denote the sets of the significant paths of \hat{h}_N^{Th} and \hat{h}_E^{Th} respectively. Deriving from (5.14), the test statistic Δ_{CIR} under H_0 has been demonstrated to follow the chi-square distribution [67],

$$H_0 : \Delta_{\text{CIR}} \sim \chi^2[0, 2(S_N \cup S_E)]. \tag{5.18}$$

Therefore the false alarm rate P_{far} , which denotes the probability of the situation that given two CIRs are from the same terminal, their difference is larger than the determination

threshold, can be given by

$$\begin{aligned} P_{far} &= P(\Delta_{CIR} > \delta_{de} | H_0) \\ &= 1 - F_{\chi^2[0,2(S_N \cup S_E)]}(\delta_{de}). \end{aligned} \quad (5.19)$$

By solving the above equation, we can get the adaptive CIR determination threshold δ_{de} as

$$\delta_{de} = \mathbf{Inv}\text{-}F_{\chi^2[0,2(S_N \cup S_E)]}(1 - P_{far}), \quad (5.20)$$

where $\mathbf{Inv}\text{-}F(\cdot)$ is the inverse function of $F(\cdot)$.

5.3.6 Details of the CIR-Based Estimation Algorithm

When implementing the proposed algorithm, initially we obtain the adaptive noise threshold θ_{th} and determination threshold δ_{de} through the off-line training based on (5.9) and (5.20). During each estimation phase, we execute the estimation process by periodically estimating the CIR h , which is then compared to the existing CIRs through the threshold δ_{th} . If none of the existing CIRs is the same as h , we count h as from a new active terminal and record it for next time comparison. Otherwise, we just ignore it.

Let H_T denote the set of the existing CIRs and n_T denote the number of terminals. Our proposed CIR-based estimation algorithm can be explained in detail as

Algorithm 1 CIR-based user number estimation

1. Initialization:

- 1) switch to the monitoring channel;
- 2) set maximum monitoring time $T_{max} = 100$;
- 3) set current monitoring time $t_{cur} = 0$;
- 4) set the number of competing terminals $n_T \leftarrow 0$.

2. While $t_{cur} \leq T_{max}$:(a) $bIsBreak \leftarrow false$ (b) Estimate the channel to get the CIR \hat{h}_c (c) Mitigate the noise according to (5.7) based on θ_{th} , that is $\hat{h}_c \rightarrow \hat{h}_c^{th}$ (d) For $i = 1$ to n_T i. calculate the CIR difference Δ_h as

$$\Delta_h \leftarrow \frac{1}{\rho^2} \sum |\hat{h}_c^{th} - H_T(i)|^2$$

ii. If $\Delta_h \geq \delta_{de}$ *continue*;

Else

 $bIsBreak = true$;(e) If $bIsBreak == false$ $n_T = n_T + 1$; $H_T(n_T) = \hat{h}_c^{th}$;(f) $t_{cur} = t_{cur} + 1$

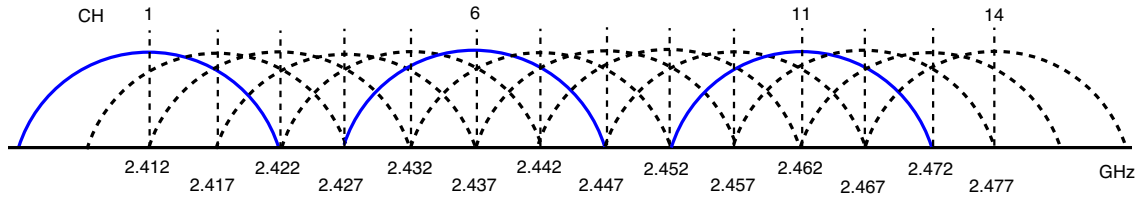


Figure 5.3: IEEE 802.11 channels in the 2.4GHz ISM band [68].

5.4 Channel Assignment Exploiting IEEE 802.11 Partially Overlapped Channels

5.4.1 Interference Analysis of Partially Overlapped Channels

In IEEE 802.11 standards, two unlicensed frequency spectrum bands are defined, those are: 1). 2.4 GHz Industrial, Scientific and Medical (ISM) band, and 2). 5 GHz Unlicensed National Information Infrastructure (UNII) band, where we consider the more widely deployed unlicensed 2.4 GHz ISM band, i.e. used in IEEE 802.11 b/g/n.

In North American, as depicted in Fig.5.3, the ISM band provides 11 channels available with the channels a 22MHz bandwidth but their central frequencies are spaced only 5MHz between neighbors. Therefore, only three of the 11 channels, namely 1, 6 and 11, are non-overlapped and the simultaneous use of them will not cause any interferences. As for the rest, they are partially overlapped and the simultaneous transmission on them with the transmission range overlap will cause the adjacent channel interferences.

In [68], a pioneer work has illustrated that the careful use of the partially overlapped channels was not always harmful while in some aspects, it could bring significant improvements in spectrum utilization and the system performance. Following this breakthrough, some further investigations were subsequently done to solve the problem of channel assignment in wireless mesh networks and WLANs, with the consideration of partially overlapped channels [69, 70, 71].

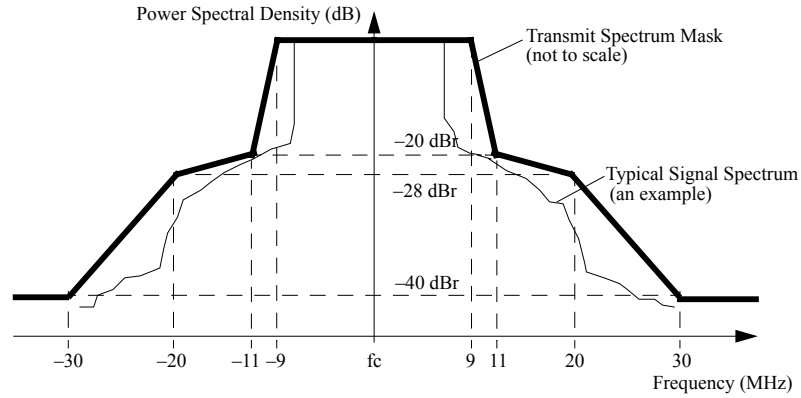


Figure 5.4: Transmit spectrum mask for IEEE 802.11 OFDM modulation.

To explore the benefits of using partially overlapped channels, we explore the Interference Factor (shortly called as I-factor, denoted by δ) in [68] to describe the amount of frequency overlap between two different channels, where the I-factor $\delta_{(i,j)}(\tau)$ represents the interference between channel i and channel j with transmission range overlap, given as

$$\delta_{(i,j)}(\tau) = \delta_{(j,i)}(\tau) = \int_{-\infty}^{+\infty} S_i(F)S_j(F - \tau)df, \quad (5.21)$$

where the impacts of the transmission range overlap are neglected and we only consider the frequency overlap for simplicity, and $\tau = |f_i - f_j|$ denotes the central frequency space between the two channels, and it can be computed as $\tau = 5|i - j|$ in MHz. As for $S_i(f)$ and $S_j(f)$, they are the signal's power distribution across the frequency spectrum in channel i and channel j respectively, where with OFDM modulation, they are determined by the transmit spectrum mask shown in Fig.5.4, and calculated as

$$S_i(f) = S_j(f) = \begin{cases} 0\text{dB}, & \text{if } |f - F_c| \leq 9 \\ -10|f| + 90\text{dB}, & \text{if } 9 < |f - F_c| \leq 11 \\ \frac{-8|f|-92}{9}\text{dB}, & \text{if } 11 < |f - F_c| \leq 20 \\ \frac{-6|f|-4}{5}\text{dB}, & \text{if } 20 < |f - F_c| \leq 30 \\ -40\text{dB}, & \text{if } |f| > 30 \end{cases}, \quad (5.22)$$

where F_c denotes the channel center frequency.

Observing from (5.21), it is evident that the I-factor between two channels can be determined only by their central frequency spaces, which can be simply represented by their index. Therefore, we re-define the I-factor $\delta_{(i,j)}(\tau)$ as $\delta(\sigma)$, where σ is given by $\sigma = |i - j|$.

5.4.2 Problem Formulation

We extend the problem in [56] to a more general scenario, that is we not only consider the limited non-overlapped channels, but also involve the partially overlapped channels. We first define the following variables:

- C is the set of available IEEE 802.11 channels.
- $\delta(\sigma)$ is the I-factor between channel i and j .
- $N(i)$ is the number of users in channel i .
- M_i is the set of neighboring channels which are partially overlapped with channel i .
- c_{ag} is the selected channel for objective AP.

As demonstrated in [56], with the purpose of maximizing the system throughput, the LS scheme in [55] can be simplified as

$$c_{ag} = \arg \min_{i \in C} N(i), \quad (5.23)$$

where it shows in order to achieve a maximum system throughput, the AP only need to choose the channel with the minimum number of users.

Taking the partially overlapped channels into consideration, we define a notion of *Equivalent User Number* (EUN) of channel i , denoted by $EUN(i)$, which combines both the number of users in channel i and the equivalent number of users from the partially overlapped channels caused by the adjacent interferences. Using the I-factor in (5.21), $EUN(i)$ can be computed as [68]

$$\begin{aligned} EUN(i) &= N(i) + \sum_{j \in M_i} (R_j \delta(|i - j|)^{1/2})^2 \phi_j \\ &= N(i) + \sum_{j \in M_i} \delta(|i - j|) \phi_j R_j^2 \\ &= N(i) + \sum_{j \in M_i} \delta(|i - j|) N(j), \end{aligned} \quad (5.24)$$

where R_j denotes the transmission range radius of the AP using channel j , and ϕ_j is the user density of that AP. With the fact that $\delta(0) = 1$ and $\delta(|i - j|) = 0$ if $j \notin M_i$, $EUN(i)$ can be simplified as

$$EUN(i) = \sum_{j \in C} \delta(|i - j|) N(j). \quad (5.25)$$

Therefore, in order to maximize the system throughput with the consideration of partially overlapped channels to solve the frequency scarcity problem, the objective problem

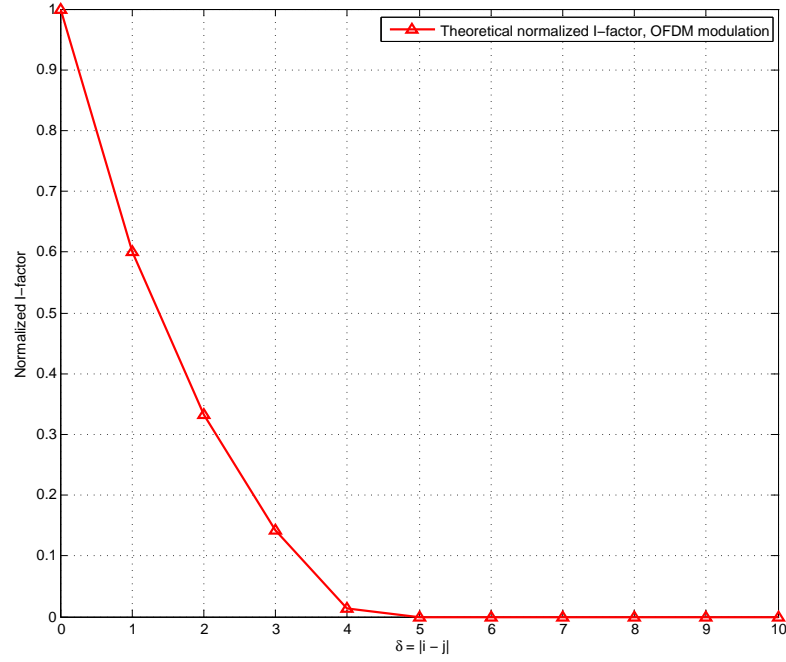


Figure 5.5: Theoretical I-factor on 2.4GHz 802.11 channels with OFDM modulation.

of our proposed channel assignment algorithm can be formulated as

$$\begin{aligned}
 c_{ag} &= \arg \min_{i \in C} EUN(i) \\
 &= \arg \min_{i \in C} \sum_{j \in C} \delta(|i - j|) N(j).
 \end{aligned} \tag{5.26}$$

5.4.3 Interference Factor (I-factor) Calculation

In practice, the amount of power received is obtained by multiplying the frequency response of the band-pass filter to the incoming signal and it is advantageous to use the same filter for both the transmitting and band-limiting reception. Thus, we consider the transceiver and receiver filter to be the same as the transmit spectrum mask shown in Fig.5.4, with the bandwidth 22MHz. By cutting off the received signal beyond the band-pass filter, the

signal's power distribution in (5.22) is re-written as

$$S_i(f) = S_j(f) = \begin{cases} 0\text{dB}, & \text{if } |f - F_c| \leq 9 \\ -10|f| + 90\text{dB}, & \text{if } 9 < |f - F_c| \leq 11 \\ -\infty\text{dB}, & \text{otherwise} \end{cases}, \quad (5.27)$$

Combining (5.21) and (5.27), the discrete I-factor for the 2.4GHz 802.11 channels with OFDM modulation can be obtained as shown in Fig.5.5, where we can see that with the increase of σ , the I-factor decreases dramatically and when $\sigma \geq 5$, no interference exists between the two channels. This explains the non-overlapped channels in IEEE 802.11, namely channel 1, 6 and 11.

5.4.4 Implementation of the Proposed Channel Assignment

Algorithm

Based on the number of users and the I-factor obtained previously, we carry out our proposed algorithm with the purpose of maximizing the system throughput as formulated in (5.26) by the following steps:

Step a: Estimate the number of users in each IEEE 802.11 channel (channel 1 to 11) using the proposed CIR-based algorithm introduced in Chapter 5.3;

Step b: Calculate the I-factor;

Step c: For each channel, with the results in **Step a** and **Step b**, calculate its EUN;

Step d: Select the channel with the minimum EUN, switch the AP to that channel and start the operating;

Step e: At the running phase, the AP keeps updating the user number in each channel and will re-execute the channel selection process **Step a - Step d** once either the EUN

Table 5.1: Simulation Parameters for User Number Estimation

Subcarrier number	52	Pilot number	4
Preamble length N_p	53	CP length N_{cp}	16
False alarm rate P_{far}	0.1	AR coefficient η	0.9
Training window size M	100	Simulation times	10000

exceeds a certain threshold or the system quality of service (QoS) drops under the users' requirements.

5.5 Simulations

5.5.1 Parameter Setting

In this section, simulations using MatLab are provided to validate the proposed algorithm. As defined in IEEE 802.11, the physical layer OFDM symbol is set to have 52 subcarriers, of which 4 are pilots that facilitate phase tracking for coherent demodulation. We first simulate the CIR estimation algorithm with the parameters listed in Table 5.1.

Then, the performance of the proposed channel assignment in terms of packet drop rate at MAC layer and the average system throughput, is given based on the MAC layer performance analysis method in [72], where we set the MAC layer queue length to be 30 and some other IEEE 802.11 system parameters are presented in Table 5.2. Moreover, we also simulate the random selection channel assignment algorithm (RS algorithm) as comparison.

5.5.2 Adaptive Noise Elimination and CIR Determination Thresholds

We begin with presenting the noise elimination threshold under different SNRs and path numbers. As shown in Fig. 5.6, the noise elimination threshold first decreases with the increase of SNR and then maintain unchanged after the SNR reaches a certain level, i.e.

Table 5.2: IEEE 802.11 System Parameters

Channel bir rate	2 Mbits/s
PHY header	192 bits
MAC header	224 bits
Packet payload size	1000 Bytes
Length of RTS	160 bits + PHY header
Length of CTS	112 bits + PHY header
Length of ACK	112 bits + PHY header
Initial backoff window size	31
Maximum backoff stages	5
Short retry limit	7
Long retry limit	4

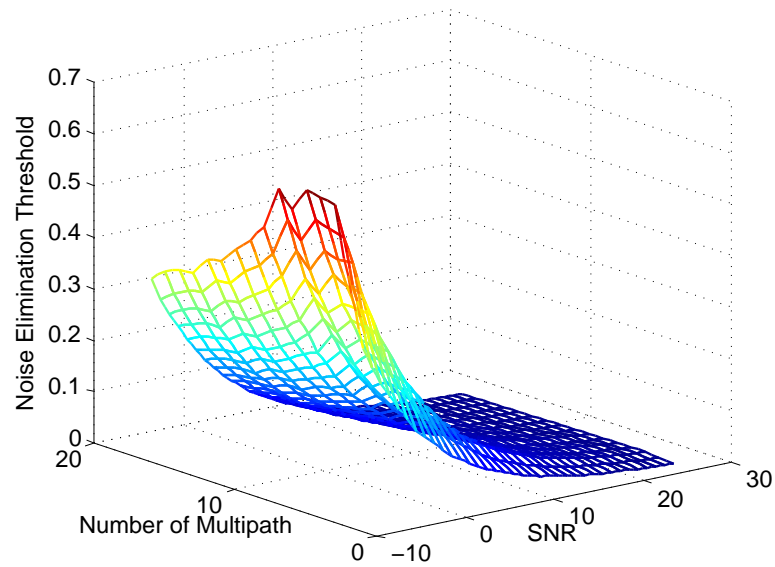


Figure 5.6: Noise elimination threshold under different path number and SNR combinations.

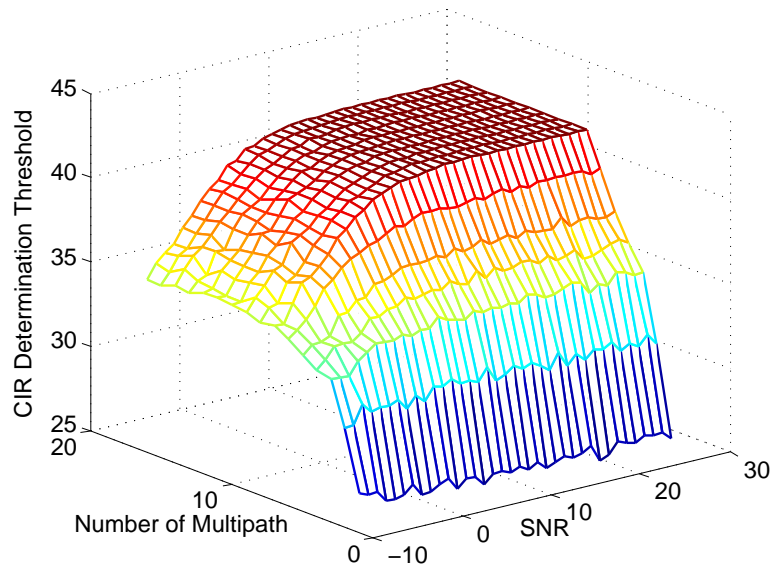


Figure 5.7: CIR determination threshold under different path number and SNR combinations.

0dB in the simulation case. Furthermore, when the SNR is low, the threshold varies with the change of path number while in high SNR condition, it keeps stable regardless of the variation of path number.

Fig. 5.7 shows the variation of the CIR determination threshold where it is easy to conclude that the threshold increases with the increase of path number and fluctuates with the change of SNR. Besides, a stable CIR determination threshold can only be achieved under large number of multipath and high SNR condition. In light of this, it is necessary to adopt the adaptive CIR determination threshold in the proposed algorithm.

5.5.3 Accuracy Analysis of CIR-based User Number Estimation

To verify the proposed CIR-based user number estimation scheme, the cumulative distribution function (CDF) of the estimation errors is shown in Fig. 5.8, where evidently, with the increase of SNR, the performance of the proposed algorithm gets better. Specifically, under a reasonable SNR condition, i.e. above 0dB, approximate 90% of the estimation errors is

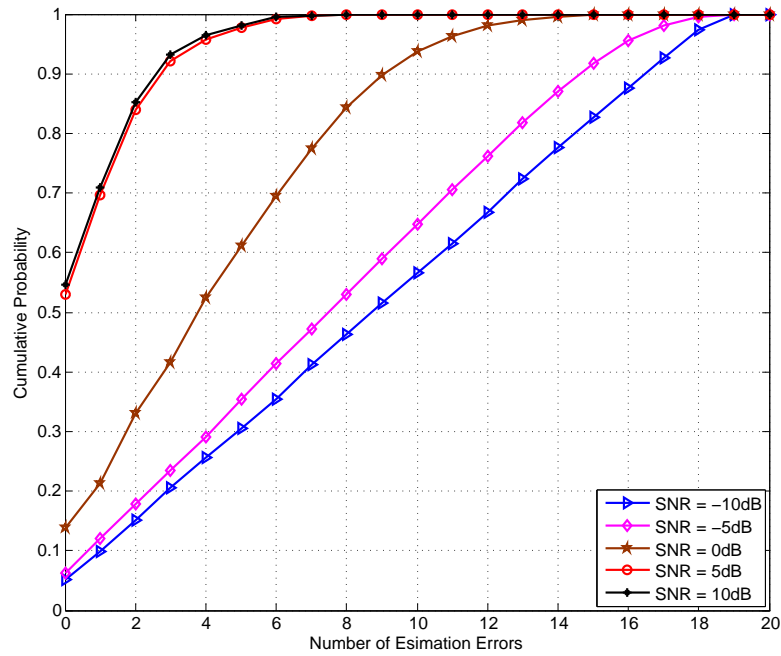


Figure 5.8: CDF of the estimation errors under different SNR situations.

below three. Therefore, using the proposed algorithm, the user number can be obtained accurately, providing the crucial information for the following channel assignment.

5.5.4 IEEE 802.11 WLAN System Performance Improvement

Then, we simulate the MAC layer packet drop rate of the proposed channel assignment scheme with the increasing packet arrival rate under different AP numbers, shown in Fig. 5.9. Generally, either the increase of packet arrival rate or a more crowded network, i.e. a larger N_{AP} , leads to the drop of more packets at MAC layer. However, our proposed algorithm can always get much smaller packet drop rate than the RS algorithm. Furthermore, with the increasing number of co-existing APs, the performance gap between the proposed algorithm and the RS scheme increases as well, indicating that our proposed algorithm can achieve more benefits in a more crowded network.

Fig. 5.10 presents the average system throughput of the newly deployed AP under

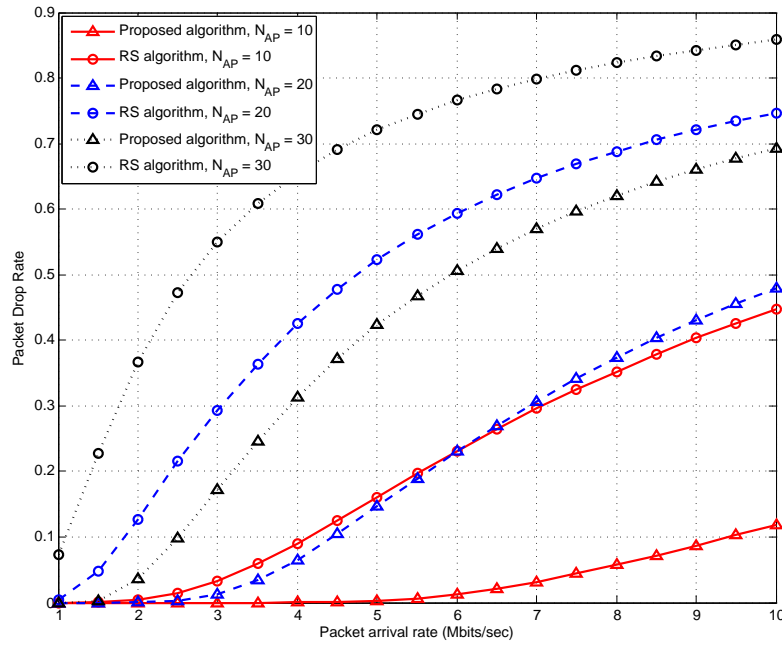


Figure 5.9: MAC layer packet drop rate under different packet arrival rates with different AP numbers.

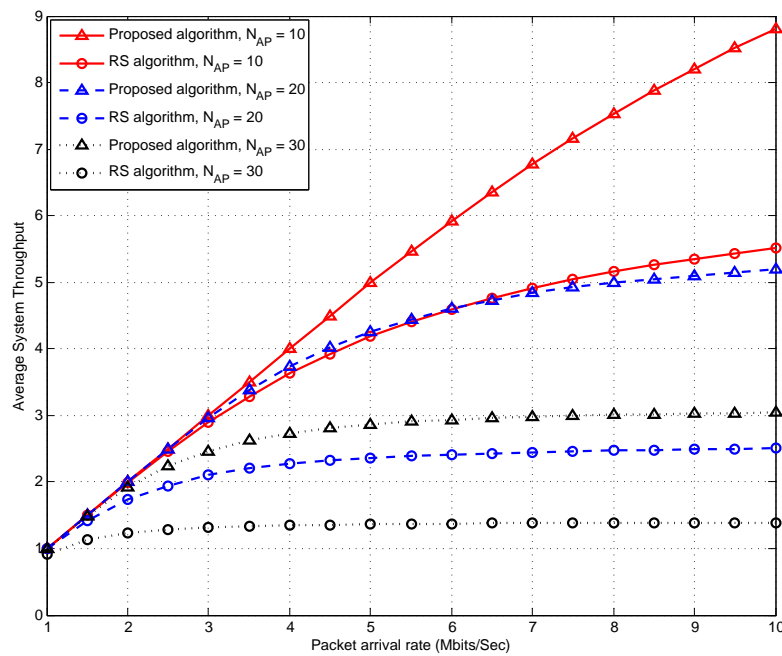


Figure 5.10: Average system throughput under different packet arrival rates with different AP numbers.

different scenarios where we can see that thanks to our throughput maximization oriented channel assignment, much higher throughput can be achieved in our proposed algorithm compared to the random channel selection. Moreover, with the increase of packet arrival rate, which means that more packets arrive during each time frame, the throughput for both two algorithms increase. Besides, as also demonstrated in Fig. 5.9, our proposed algorithm can achieve a higher system performance gains compared with the RS scheme in a more crowded area.

5.6 Summary

To improve the system throughput as well as solving the problem of frequency scarcity in dense IEEE 802.11 WLANs, a channel assignment scheme which exploited the partially overlapped channels, was proposed in this chapter. We first obtained the user number in each IEEE 802.11 channel through determining the number of different CIRs, while reducing the time responsiveness simultaneously. An adaptive noise elimination threshold was applied to mitigate the impact of CIR estimation noise. Moreover, to further improve the estimation performance, we employed an adaptive CIR determination threshold when differentiating the noise-mitigated CIRs.

Based on the obtained user number information, the IEEE 802.11 channels were then assigned to the APs, aiming at maximizing the system throughput where we took all the partially overlapped channels into consideration, and the interferences between those channels were carefully analyzed.

Simulation results demonstrated that the proposed user number estimation algorithm could achieve very high accuracy and using the proposed channel assignment scheme, the system performance could be significantly improved.

Chapter 6

Conclusion and Future Work

6.1 Conclusion

In this thesis, with the purpose of guaranteeing QoS in wireless communications, three main contributions have been made, including the multiple queue finite state Markov chain system model, the cross-layer subcarrier allocation in MU-OFDM system with QoS constraints and the QoS oriented channel assignment in IEEE 802.11 WLANs with novel user number estimation at physical layer.

More specifically, we have first extended the conventional single queue finite state Markov chain system model to multiple queues' scenario to provide diverse QoS in wireless communications. The physical layer channel was modeled by FSMC and combined with MAC layer queue status to construct the Markov chain system model. By introducing the priority-based rate allocation (PRA) algorithm, different queues were assigned with different priorities, leading to the provision of diverse QoS in wireless communications.

Secondly, the subcarrier allocation in MU-OFDM system was investigated, where we have proposed a two-step cross-layer subcarrier allocation algorithm under the constraints of MAC layer diverse QoS. The queue behavior at MAC layer was modeled by a finite state Markov chain to transform MAC layer QoS constraints to the minimum data rate requirement at physical layer for each user. The subcarrier algorithm was then conducted with the constraint of minimum data rate of each user, such that MAC layer diverse QoS requirements could be satisfied.

Finally, the channel assignment in IEEE 802.11 WLAN was studied. A user number estimation algorithm based on the CIR at physical layer was proposed to determine the number of users in IEEE 802.11 channels. To further improve the estimation accuracy, adaptive noise elimination and CIR determination threshold have also been introduced. Then, with the information of user number in each channel, a QoS oriented channel assignment algorithm was proposed where partially overlapped IEEE 802.11 channels were considered for additional frequency resources. The interferences between the partially overlapped channels have been mathematically analyzed and involved in the channel assignment. Moreover, to maintain the system QoS, users' QoS requirements were adopted to trigger the channel assignment process.

6.2 Future Work

There still remain many research potentials undisclosed in present works, which are worthwhile for further investigations. Some of them are described as follows:

- In the proposed multiple queue finite state Markov chain system model, with the increase of the queue number, the computational complexity increases as well. Therefore, reducing the computing time of the algorithm is necessary and imperative, especially when a large number of queues are deployed at MAC layer.
- When we conducted the subcarrier allocation in MU-OFDM system, the power allocation was separately considered, which resulted in the degradation of the system performance. In future research, further improvements can be achieved if the subcarrier allocation and power allocation can be jointly considered, where nevertheless reducing the algorithm complexity is still an issue for practical implementation.

-
- Only the channel impulse response (CIR) which indicates the users' physical location information, were adopted to distinguish the users. Some other information, such as the carrier frequency offset (CFO) which is determined by the hardware characteristic of the user can also be involved in the user number estimation since no two users can strictly have the same hardware parameter and thus, their CFOs should be different as well. By combining the CIR and CFO together, the estimation accuracy could be further improved.
 - Only simulations using Matlab have been conducted to verify the proposed channel assignment algorithm. A test-bed in IEEE 802.11 hardware would be helpful to find out more practical issues and further improve the algorithm.

References

- [1] R. Berezdivin, R. Breining, and R. Topp, "Next-generation wireless communications concepts and technologies," *IEEE Commun. Mag.*, vol. 40, no. 3, pp. 108-116, Mar. 2002
- [2] Ng Chee-Hock and Soong Boon-Hee, *Queueing Modelling Fundamentals*, 2nd ed. John Wiley & Sons, Ltd, 2008.
- [3] David G Kendall, *Stochastic Processes Occurring in the Theory of Queues and their Analysis by the Method of the Imbedded Markov Chain*, 1953.
- [4] S. Weinstein and P. Ebert, "Data transmission by frequency-division multiplexing using discrete Fourier transform," *IEEE Trans. on Commun. Tech.*, vol. 19, no. 5, pp. 628-634, Oct. 1971
- [5] Y. Li and G. L. Stuber, *Orthogonal Frequency Division Multiplexing for Wireless Communications*, Springer, 2005
- [6] "Wikipedia: Dirac delta function," [http : //en.wikipedia.org/wiki/Dirac_delta_function](http://en.wikipedia.org/wiki/Dirac_delta_function).
- [7] R. Prasad, *OFDM for Wireless Communication Systems*, Artech House, Inc., 2004.
- [8] H. Zhou, "Synchronization in OFDM systems," PHD's thesis, EE Department, University of Notre Dame, Notre Dame, Indiana, Apr. 2007.
- [9] T. Pollet, M. Van Bladel, and M. Moeneclaey, "BER sensitivity of OFDM systems to carrier frequency offset and Weiner phase noise," *IEEE Tran. on Commum.*, vol. 43, pt. 1, pp. 191-193, Feb.-Apr. 1995
- [10] "Wikipedia: Wireless LAN," [http : //en.wikipedia.org/wiki/Wireless_LAN](http://en.wikipedia.org/wiki/Wireless_LAN).
- [11] ETSI. "Broadband radio access networks (BRAN); HIPERLAN type 2 technical specification; physical (PHY) layer," August 2000.

- [12] IEEE standard 802.11. "Wireless LAN Medium Access Control (MAC) and Physical layer (PHY) specifications," August 1999.
- [13] H. H. Banaser, "High performance WLAN using smart antenna," PHD's thesis, ECE Department, University of Waterloo, Waterloo, Ontario, Canada, 2007.
- [14] "IEEE 802.11a. High Speed Physical Layer in the 5 GHz band. Supplement to Standard IEEE 802.11", *IEEE* New York, 1999.
- [15] W. Fahs, B. Bakhache, M. Misson and F. Jacquet "Study of a wireless medium access method inspired from PCF for industrial applications," in *Proc. ICTTA 2006*, pp. 2709-2713, Oct. 2006
- [16] Z. Chen and A. Khokhar, "Improved MAC protocols for DCF and PCF modes over fading channels in wireless LANs," in *Proc. WCNC*, vol. 2, pp. 1297-1302, Mar. 2003
- [17] D. Qiao, S. Choi. A. Soomro and K. G. Shin, "Energy-efficient PCF operation of IEEE 802.11a wireless LAN," in *Proc. Infocom*, vol. 2, pp. 580-589, Nov. 2002
- [18] K. Xu, M. Gerla, and S. Bae, "Effectiveness of RTS/CTS handshake in IEEE 802.11 based adhoc networks," *Ad Hoc Network Journal*, vol. 1, pp. 107-123, Jul. 2003.
- [19] F. Liu, J. Lin, Z. Tao and T. Korakis etc., "The hidden cost of hidden terminals," in *Proc. IEEE ICC*, pp. 1-6, May 2010.
- [20] V. Srivastava and M. Motani, "Cross-layer design: a survey and the road ahead," *IEEE Commun. Magazine*, vol. 43, no. 12, pp. 112-119, Dec. 2005.
- [21] S. Choi and K. G. Shin, "An uplink CDMA system architecture with diverse QoS guarantees for heterogeneous traffic," *IEEE/ACM Trans. Networking*, vol. 7, no. 5, pp. 616-628, Oct. 1999.
- [22] P. Mi and X. Wang, "Cross-layer dynamic subcarrier allocation in multiuser OFDM system with MAC layer diverse QoS constraints," in *Proc. IEEE PIMRC*, Sept. 2011.
- [23] P. Mi, X. Wang and M. A. Khan, "Diverse QoS support in multimedia communication with multiple MAC layer queues using FSMC," in *Proc. IEEE GLOBECOM*, Dec. 2011.

- [24] J. Tang and X. Zhang, "Cross-layer design of dynamic resource allocation with diverse QoS guarantees for MIMO-OFDM wireless networks," in *Proc. IEEE WoW-MoM*, Jun. 2005.
- [25] H. S. Wang and N. Moayeri, "Finite-state Markov channel – A useful model for radio communication channels," *IEEE Trans. Veh.Technol.*, vol. 44, no. 1, pp. 163-171, Feb. 1995.
- [26] Q. Zhang and S. A. Kassam, "Finite-state Markov model for Rayleigh fading channels," *IEEE Trans. commun.*, vol. 47, no. 11, pp. 1688-1692, Nov. 1999.
- [27] J. G. Ruiz, B. Soret, M. C. Aguayo-Torres and J. T. Entrambasaguas, "On Finite state Markov chains for Rayleigh channel modeling," s
- [28] M. S. Alouini and A. J. Glodsmith, "Adaptive modulation over Nakagami fading channels," *J. Wireless Commun.*, vol. 13, no. 1-2, pp. 119-143 May 2000.
- [29] Q. Liu, S. Zhou and G. B. Giannakis, "Queuing with adaptive modulation and coding over wireless links: Cross-Layer Analysis and Design," *IEEE Trans. Wireless commun.*, vol. 4, no. 3, pp. 1142-1153, May 2005.
- [30] X. Bai, A. Shami and S. L. Primak, "Optimal power control over fading channel with cross-layer performance constraint," in *Proc. IEEE ICC*, May 2009.
- [31] J. Gong, S. Zhou and Z. Niu, "Queuing on energy-efficient wireless transmissions with adaptive modulation and coding," in *Proc. IEEE ICC*, May 2011.
- [32] Q. Liu, X. Wang and G. B. Giannakis, "A cross-layer scheduling algorithm with QoS support in wireless networks," *IEEE Trans. Veh.Technol.*, vol. 55, no. 3, pp. 1142-1153, May 2006.
- [33] —, "Cross-layer scheduling with prescribed QoS guarantees in adaptive wireless networks," *IEEE Journal on Selected Areas in Commun.*, vol. 23, no. 5, pp. 1056-1066, May 2005.
- [34] X. Peng, M. Song and J. Song, "Cross-layer design for adaptive modulation and coding with hybrid ARQ," in *Proc. MAPE for Wireless Commun.*, pp. 138-141, Aug. 2007

- [35] M. Sherman, "IEEE standards supporting cognitive radio and networks, dynamic spectrum access, and coexistence," *Electronics and Integrated Solutions*, Jul. 2008
- [36] S. H. O. Salih and M. M. A. Suliman, "Implementation of adaptive modulation and coding techniques using Matlab," in *Proc. ELMAR 2011*, pp. 137-139, Sept. 2011
- [37] B. Sklar, "Rayleigh fading channel in mobile digital communication system part I: Characterization," *IEEE Commun. Magazine*, vol. 35, Issue 7, pp. 90-100, Jul. 1997.
- [38] J. N. A. Salazar, "802.11 Markov channel modeling," PHD's thesis, School of Information Sciences, University of Pittsburgh, Sept. 2000.
- [39] J. Arauz and P. Krishnamurthy, "A study of different partitioning schemes in first order markovian models for Rayleigh fading channels," in *Proc. IEEE WPMC*, Oct. 2002, pp.277-281.
- [40] D. Bertsekas and R. Gallager, *Data Networks*, 2nd ed. Englewood Cliffs, N.J.:Prentice Hall, 1992.
- [41] E. Lawrey, "Multiuser OFDM," *International Symposium on Signal Processing and its Applications*, pp. 761-764, Brisbane, Australia, Aug. 1999.
- [42] S. Sadr, A. Anpalagan and K. Raahemifar "Radio resource allocation algorithm for the downlink of multiuser OFDM communication systems," *Commun. Surveys Tuts.*, vol. 11, no. 3, pp. 92-106, 3rd Quar., 2009.
- [43] K. B. Letaief and Y. Zhang, "Dynamic multiuser resource allocation and adaptation for wireless systems," *IEEE Wireless Commun. Mag.*, vol. 13, no. 4, pp. 38-47, Aug., 2006.
- [44] C. Y. Wong, R. S. Cheng, K. B. Letaief and R. D. Murch "Multiuser OFDM with adaptive subcarrier, bit, and power allocation," *IEEE J. Sel. Areas Commun.*, vol. 17, no. 10, pp. 1747-1758, Oct., 1999.
- [45] W. Rhee and J. M. Cioffi, "Increasing in capacity of multiuser OFDM system using dynamic subchannel allocation," *IEEE J. Sel. Area Commun.*, vol. 21, no. 2, pp. 171-178, Feb. 2003.

- [46] J. Jang and K. B. Lee, "Transmit power adaptation for multiuser OFDM systems," *IEEE J. Sel. Area Commun.*, vol. 21, no. 2, pp. 171-178, Feb. 2003.
- [47] W. Xu, C. Zhao, P. Zhou and Y. J. Yang "Efficient adaptive resource allocation for multiuser OFDM systems with minimum rate constraints," in *Proc. IEEE ICC*, pp. 5126-5131, Aug. 2007.
- [48] A. Falahati and M. R. Ardestani, "An improved low-complexity resource application algorithm for OFDMA systems with proportional data rate constraint," in *Proc. IEEE ICACT*, pp. 606-610, May. 2007.
- [49] G. Song and Y. G. Li, "Utility-based joint physical-MAC layer optimization in OFDM," in *Proc. IEEE Globecom*, vol. 1, pp. 671-675, Nov. 2002.
- [50] Z. Shen, J. G. Andrews and B. L. Evans, "Adaptive resource allocation in multiuser OFDM systems With proportional rate constraints," *IEEE Trans. Wireless commun.*, vol. 4, no. 6, pp. 2726-2737, Nov. 2005.
- [51] T. S. Rappaport, *Wireless Communications: Principles and Practice*, Upper Saddle River, N.J.:Prentice Hall, 2002.
- [52] S. Chiochan, E. Hossain, and J. Diamond, "Channel assignment schemes for infrastructure-based 802.11 WLANs: A survey," *IEEE Comm. Survey & Tutorials*, vol. 12, no. 1, pp. 124-136, 2010.
- [53] P. Mahonen, J. Riihijarvi, and M. Petrova, "Automatic channel allocation for small wireless local area networks using graph colouring algorithm approach," in *Proc IEEE PIMRC 2004*, vol. 1, pp. 536-539, Sept. 2004.
- [54] D. Fan, X. Wang, and P. Mi, "Cross-Layer Interference Minimization-Oriented Channel Assignment in IEEE 802.11 WLANs," in *Proc IEEE PIMRC 2011*, pp. 1083-1087, Sept. 2011.
- [55] H. Luo and N. K. Shankaranarayanan, "A distributed dynamic channel allocation technique for throughput improvement in a dense WLAN environment," in *Proc IEEE ICASSP*, V-345-8 vol. 5, May 2004.
- [56] M. Driberg, F. -C. Zheng, and R. Ahmad, "Minimum neighbour and extended Kalman filter estimator: a practical distributed channel assignment scheme for

- dense wireless local area networks,” *IET Communications*, vol. 4, no. 15, pp. 1865-1875, Oct. 2010.
- [57] A. L. Toledo, T. Vercauteren, and X. Wang, “Adaptive optimization of IEEE 802.11 DCF based on bayesian estimation of the number of competing terminals,” *IEEE Trans. on Mobile Computing*, vol. 5, no. 9, pp. 1283-1296, Sept. 2006.
- [58] G. Bianchi and I. Tinnirello, “Kalman filter estimation of the number of competing terminals in an IEEE 802.11 network,” in *Proc. INFOCOM 2003*, vol. 2, pp. 844-852, Mar. 2003
- [59] T. Vercauteren, A. L. Toledo and X. Wang, “Batch and Sequential Bayesian Estimators of the Number of Active Terminals in an IEEE 802.11 Network,” *IEEE Trans. on Signal Processing*, Vol. 55, No. 2, pp. 437-450, Feb. 2007.
- [60] “IEEE 802.11a. High Speed Physical Layer in the 5 GHz band. Supplement to Standard IEEE 802.11”, *IEEE New York*, 1999.
- [61] “Wikipedia: Heaviside step function,” [http : //en.wikipedia.org/wiki/Heaviside_step_function](http://en.wikipedia.org/wiki/Heaviside_step_function).
- [62] M. Hsieh and C. Wei, “Channel estimation for OFDM systems based on comb-type pilot arrangement in frequency selective fading channels,” *IEEE Trans. Consumer Electron*, Vol. 44, pp. 217-225, Feb. 1998.
- [63] N. Patwari, and S. K. Kasera, “Temporal link signature measurements for location distinction,” *IEEE Trans. on Mobile Computing*, Vol. 10, no. 11, Mar. 2011.
- [64] S. Rosati, G. E. Corazza and A. V. -Coralli, “OFDM channel estimation with optimal threshold-based selection of CIR samples,” in *Proc. GLOBECOM 2009*, pp. 1-7, Dec. 2009.
- [65] F. -X. Socheleau, A. A. -El-Bey and S. Houcke, “Non data-aided SNR estimation of OFDM signals,” in *IEEE Comm. Letters*, vol.12, pp. 813-815, Nov. 2008.
- [66] L. Xiao, L. J. Greenstein, N. B. Mandayam and W. Trappe, “Using the physical layer for wireless authentication in time-variant channels,” *IEEE Trans. Inf. Theory*, vol. 46, no. 4, pp. 1350-1356, Jul. 2000.

-
- [67] F. Liu, X. Wang and H. Tang, "Robust physical layer authentication using inherent properties of channel impulse response," in *Proc. MILCOM 2011*, Nov. 2011.
- [68] A. Mishra, V. Shrivastava, S. Banerjee, and W. Arbaugh, "Partially overlapped channels not considered harmful," *SIGMETRICS Perform. Eval. Rev.*, 34(1), 2006.
- [69] Z. Feng and Y. Yang, "How much improvement can we get from partially overlapped channels" in *Proc IEEE WCNC 2008*, pp. 2957-2962, 2008.
- [70] Y. Liu, R. Venkatesan and C. Li, "Channel assignment exploiting partially overlapping channels for wireless mesh networks" in *Proc IEEE GLOBECOM 2009*, pp. 1-5, Dec. 2009.
- [71] R. Akl and A. Arepally, "Dynamic channel assignment in IEEE 802.11 networks" in *Proc IEEE PORTABLE07*, pp. 1-5, May 2007.
- [72] H. Zhai, Y. Jwon and Y. Fang, "Performance analysis of IEEE 802.11 MAC protocols in wireless LANs," *Wireless Communications and Mobile Computing*, vol. 4, no. 8, pp. 917-931, 2004.

Curriculum Vitae

Name: Penghui Mi

Place of birth: Chongqing, P. R. China

Year of birth: 1986

Post-secondary Education and Degrees:

2010–2012, Candidate, Master of Engineering Science
Faculty of Engineering
The University of Western Ontario
London, Ontario, Canada

2004–2008, Bachelor of Science
Department of Electronic and Science and Technology
University of Science and Technology of China
Hefei, Anhui, P.R.China

Publications:

- [1] P. Mi and X. Wang, “Improved channel assignment for WLANs by exploiting partially overlapped channels with novel CIR-based user number estimation,” to appear in *Proc. IEEE ICC workshop*, Jun. 2012.
- [2] P. Mi, X. Wang and M. Khan, “Diverse QoS support in multimedia communication with multiple MAC layer queues using FSMC,” in *Proc. IEEE GLOBECOM*, Dec. 2011.
- [3] P. Mi and X. Wang, “Cross-layer dynamic subcarrier allocation in multiuser OFDM system with MAC layer diverse QoS constraints,” in *Proc. IEEE PIMRC*, Sept. 2011.
- [4] D. Fan, X. Wang and P. Mi, “Cross-layer interference minimization-oriented channel assignment in IEEE 802.11 WLANs,” in *Proc. IEEE PIMRC*, Sept. 2011.
- [5] D. Fan, X. Wang and P. Mi, “Distributed self-optimization for efficient reconfiguration in overlapping heterogeneous wireless access networks,” in *Proc. IEEE PIMRC workshop*, Sept. 2011.